Histone methyltransferase activity of a Drosophila Polycomb group repressor complex. *Cell* **111**, 197-208.
Nichols, J., Zevnik, B., Anastassiadis, K., Niwa, H., Klewe-Nebenius, D., Chambers, I., Scholer, H. and Smith, A. (1998). Formation of pluripotent stem cells in the mammalian embryo depends on the POU transcription factor Oct4. *Cell* **95**, 379-391.
Niwa, H., Miyazaki, J. and Smith, A. G. (2000). Quantitative expression of Oct-3/4 defines differentiation, dedifferentiation or self-renewal of ES cells. *Nat. Genet.* **24**, 372-376.
Niwa, H., Toyooka, Y., Shimosato, D., Strumpf, D., Takahashi, K., Yagi, R. and Rossant, J. (2005). Interaction between Oct3/4 and Cdx2 determines trophectoderm differentiation. *Cell* **123**, 917-929.
Ohta, H., Sawada, A., Kim, J. Y., Tokimasa, S., Nishiguchi, S., Humphries, R. K., Hara, J. and Takihara, Y. (2002). Polycomb group gene rae28 is required for sustaining activity of hematopoietic stem cells. *J. Exp. Med.* **195**, 759-770.
Okumura-Nakanishi, S., Saito, M., Niwa, H. and Ishikawa, F. (2005). Oct-3/4 and Sox2 regulate Oct-3/4 gene in embryonic stem cells. *J. Biol. Chem.* **280**, 5307-5317.
Orlando, V., Strutt, H. and Paro, R. (1997). Analysis of chromatin structure by in vivo formaldehyde cross-linking. *Methods* **11**, 205-214.
Park, I. K., Qian, D., Kiel, M., Becker, M. W., Pihalja, M., Weissman, I. L., Morrison, S. J. and Clarke, M. F. (2003). Bmi-1 is required for maintenance of adult self-renewing haematopoietic stem cells. *Nature* **423**, 302-305.
Rodda, D. J., Chew, J. L., Lim, L. H., Loh, Y. H., Wang, B., Ng, H. H. and Robson, P. (2005). Transcriptional regulation of nanog by OCT4 and SOX2. *J. Biol. Chem.* **280**, 24731-24737.
Seibler, J., Zevnik, B., Kuter-Luks, B., Andreas, S., Kern, H., Hennek, T., Rode, A., Heimann, C., Faust, N., Kauselmann, G. et al. (2003). Rapid generation of inducible mouse mutants. *Nucleic Acids Res.* **31**, e12.
Shao, Z., Raible, F., Mollaaghababa, R., Guyon, J. R., Wu, C. T., Bender, W. and Kingston, R. E. (1999). Stabilization of chromatin structure by PRC1, a Polycomb complex. *Cell* **98**, 37-46.
Shimosato, D., Shiki, M. and Niwa, H. (2007). Extra-embryonic endoderm cells derived from ES cells induced by GATA Factors acquire the character of XEN cells. *BMC Dev Biol.* **7**, 80.
Villa, R., Pasini, D., Gutierrez, A., Morey, L., Occhionorelli, M., Vire, E., Nomdedeu, J. F., Jenuwein, T., Pelicci, P. G., Minucci, S. et al. (2007). Role of the polycomb repressive complex 2 in acute promyelocytic leukemia. *Cancer Cell* **11**, 513-525.
Wang, H., Wang, L., Erdjument-Bromage, H., Vidal, M., Tempst, P., Jones, R. S. and Zhang, Y. (2004). Role of histone H2A ubiquitination in Polycomb silencing. *Nature* **431**, 873-878.
Wang, J., Rao, S., Chu, J., Shen, X., Levasseur, D. N., Theunissen, T. W. and Orkin, S. H. (2006). A protein interaction network for pluripotency of embryonic stem cells. *Nature* **444**, 364-368.
Williams, R. L., Hilton, D. J., Pease, S., Willson, T. A., Stewart, C. L., Gearing, D. P., Wagner, E. F., Metcalf, D., Nicola, N. A. and Gough, N. M. (1988). Myeloid leukaemia inhibitory factor maintains the developmental potential of embryonic stem cells. *Nature* **336**, 684-687.
Wysocka, J., Myers, M. P., Laherty, C. D., Eisenman, R. N. and Herr, W. (2003). Human Sin3 deacetylase and trithorax-related Set1/Ash2 histone H3-K4 methyltransferase are tethered together selectively by the cell-proliferation factor HCF-1. *Genes Dev.* **17**, 896-911.

Netrin-1 acts as a survival factor for aggressive neuroblastoma

Céline Delloye-Bourgeois,[1] Julien Fitamant,[1] Andrea Paradisi,[1] David Cappellen,[2] Setha Douc-Rasy,[2] Marie-Anne Raquin,[3] Dwayne Stupack,[4] Akira Nakagawara,[5] Raphaël Rousseau,[6] Valérie Combaret,[6] Alain Puisieux,[6] Dominique Valteau-Couanet,[3] Jean Bénard,[2] Agnès Bernet,[1] and Patrick Mehlen[1]

[1]Apoptosis, Cancer and Development Laboratory, Equipe labellisée 'La Ligue', Centre National de la Recherche Scientifique UMR5238, Université de Lyon, 69008 Lyon, France
[2]Molecular Interactions and Cancer Centre, National de la Recherche Scientifique UMR 8126 and IFR54, and [3]Oncopediatric Department, Gustave Roussy Institute, 94805 Villejuif Cedex, France
[4]Department of Pathology, School of Medicine, Moores Cancer Center, University of California, San Diego, La Jolla, CA 92093
[5]Division of Biochemistry, Chiba Cancer Center Research Institute, Chiba 260-8717, Japan
[6]Institut National de la Santé et de la Recherche Médicale U590, Unité d'Oncologie Moléculaire, Université de Lyon, 69008 Lyon, France

Neuroblastoma (NB), the most frequent solid tumor of early childhood, is diagnosed as a disseminated disease in >60% of cases, and several lines of evidence support the resistance to apoptosis as a prerequisite for NB progression. We show that autocrine production of netrin-1, a multifunctional laminin-related molecule, conveys a selective advantage in tumor growth and dissemination in aggressive NB, as it blocks the proapoptotic activity of the UNC5H netrin-1 dependence receptors. We show that such netrin-1 up-regulation is a potential marker for poor prognosis in stage 4S and, more generally, in NB stage 4 diagnosed infants. Moreover, we propose that interference with the netrin-1 autocrine loop in malignant neuroblasts could represent an alternative therapeutic strategy, as disruption of this loop triggers in vitro NB cell death and inhibits NB metastasis in avian and mouse models.

CORRESPONDENCE
Patrick Mehlen:
mehlen@lyon.fnclcc.fr

Abbreviations used: CAM, chorioallantoic membrane; DAPK, DAP kinase; DCC, deleted in colorectal cancer; MNA, *MYCN* amplification; mRNA, messenger RNA; Myoc, myocardium; NB, neuroblastoma; PTX, primary tumor xenograft; Q-RT-PCR, quantitative RT-PCR; siRNA, small interfering RNA; TUNEL, terminal deoxynucleotidyl transferase–mediated dUTP-biotin nick end labeling.

Dependence receptors now number more than a dozen, including deleted in colorectal cancer (DCC) (1), UNC5H (2), Patched (3), some integrins (4), neogenin (5), $p75^{NTR}$ (6), RET (7), ALK (8), and TrkC (9). Although they have no structural homology (other than possibly in a domain referred to as the DART [dependence-associated receptor transmembrane] domain) (10), they all share the functional property of inducing cell death when disengaged from their trophic ligands, whereas the presence of their trophic ligands blocks this proapoptotic activity. Such receptors thus create cellular states of dependence on their respective ligands (11, 12).

The prototype dependence receptors are the netrin-1 receptors. Netrin-1, a diffusible laminin-related protein, has been shown to play a major role in the control of neuronal navigation during the development of the nervous system by interacting with its main receptors, DCC (13, 14, 15) and UNC5H (16, 17). However, DCC and UNC5H (i.e., UNC5H1, UNC5H2, UNC5H3, and UNC5H4) have been shown to belong to the dependence receptor family (1, 2). This dependence effect upon netrin-1 has been suggested to act as a mechanism for eliminating tumor cells that would develop in settings of ligand unavailability (for reviews see references 18, 19). Along this line, disruption of the proapoptotic signaling of these netrin-1 receptors in the gastrointestinal tracts of mice, by netrin-1 overexpression or by inactivation of UNC5H3, is associated with intestinal tumor progression (20, 21).

Thus, loss of the dependence receptors' proapoptotic activity represents a selective advantage for tumor cells. In this respect, DCC was proposed in the early 1990s to function as a tumor suppressor gene, whose expression is lost in

J. Bénard, A. Bernet, and P. Mehlen contributed equally to this paper.

The Rockefeller University Press $30.00
J. Exp. Med. Vol. 206 No. 4 833-847
www.jem.org/cgi/doi/10.1084/jem.20082293

the vast majority of human cancers (22, 23). This hypothesis also fits with the observation that UNC5H genes are down-regulated in most colorectal tumors, hence suggesting that loss of UNC5H genes represents a selective advantage for tumor development (21, 24, 25). We have analyzed expression of netrin-1 and its receptors in neuroblastoma (NB), the most frequent extracranial solid tumor of early childhood. The aggressive and metastatic stage 4 NB displays three distinct clinical patterns at presentation and dissemination sites based on patients' ages. Indeed, neonates and infants (<1 yr of age) with stage 4S and stage 4 without 4S features have an overall good prognosis, whereas stage 4 in children (>1 yr of age) shows a poor prognosis. We describe in this paper that, rather than the loss of netrin-1 receptor expression, a large fraction of aggressive NBs has evolved to select a gain of ligand expression that apparently represents a similar selective growth advantage. We therefore propose to use disruption of this selective advantage as an anti-cancer strategy in NB.

RESULTS

Netrin-1 is up-regulated in a large fraction of aggressive NB

We focused on stage 4 NB with a specific interest in comparing netrin-1 and its receptors' expression levels between the three distinct clinical patterns of stage 4, based on disease distribution and age of the patients (26). On the one hand, there are the neonates and infants (<1 yr of age) with stage 4S (2–5% of all NB) and the similarly young stage 4 without 4S features, hereafter termed [1yr$^-$] stage 4, who make up 10% of the NB population. On the other hand, there are the stage 4 children (>1 yr of age), comprising 45% of all NBs, who will hereafter be termed [1yr$^+$] stage 4. These three clinical aspects of stage 4 NB differ in their respective malignant behaviors and associated prognoses: good for stage 4S and [1yr$^-$] stage 4 (5-yr event-free survival >80%), and dismal for [1yr$^+$] stage 4 (5-yr event-free survival of ~30%) despite intensive treatment including high-dose chemotherapy and hematopoietic stem cell transplantation (27, 28).

We first analyzed the expression of netrin-1 and its dependence receptors, DCC, UNC5H1, UNC5H2, UNC5H3, and UNC5H4, by quantitative RT-PCR (Q-RT-PCR) in a panel of 102 stage 4 NB tumors including 24 stage 4S and 12 [1yr$^-$] stage 4. As shown in Fig. 1 A, netrin-1 is up-regulated in [1yr$^+$] stage 4 as compared with both stage 4S ($P < 0.05$) and [1yr$^-$] stage 4 ($P < 0.01$). Similar results were obtained when comparing netrin-1 protein level by immunohistochemistry (Fig. 1 B and quantification in Fig. S1 A). Interestingly, netrin-1 is detected mainly in tumor cells and is barely detected in stroma cells (Fig. 1 B and Fig. S1 B). Conversely, netrin-1 dependence receptor expression analysis showed that DCC was only weakly expressed in the different stage 4 NB (Fig. S1 C) as reported (29), whereas UNC5H1, UNC5H2, UNC5H3, and UNC5H4 expression showed no significant differences when comparing [1yr$^-$] versus [1yr$^+$] stage 4 (Fig. 1 C). However, we observed that the different UNC5H receptors are up-regulated specifically in stage 4S (mean increase in UNC5H expression in stage 4S vs. other stage 4 NBs: 2.98-fold, $P < 0.007$), suggesting UNC5H receptors as hallmarks of stage 4S NB. The UNC5H1 and UNC5H4, which show the highest messenger RNA (mRNA) expression, could also be seen at the protein level by immunohistochemistry (Fig. 1 D).

In an attempt to correlate netrin-1 up-regulation with the molecular signature of these tumors, we compared netrin-1 up-regulation and DCC/UNC5H1 levels to the profile of gene expression performed in a small panel of nine stage 4 NBs (30). We failed to detect any correlation between netrin-1 up-regulation or DCC/UNC5H1 levels with the molecular signature of apoptosis or invasion effectors (Fig. S1 D). Considering patients' outcomes, although 38% of [1yr$^+$] stage 4 NBs have selected up-regulation of netrin-1, this event failed to be significantly associated with poor outcome in this aggressive form of the disease (unpublished data). Moreover no association between netrin-1 up-regulation and *MYCN* amplification (MNA) was detected (unpublished data). Thus, netrin-1 up-regulation may be considered as an additional component of the genetic complexity that these tumors display.

Despite a largely favorable prognosis among infants with stage 4 NB (i.e, stage 4S and [1yr$^-$] stage 4) with no MNA, many succumb to the disease. Thus, we assessed whether netrin-1 expression may serve as a prognostic marker for the infants with stage 4 NB. As shown in Fig. 1 E, the overall survival of infants with stage 4S differed markedly based on whether the tumor displayed high levels of netrin-1 expression (netrin-1 high) or low-level expression (netrin-1 low), with the netrin-1 expression threshold being its median expression value in the 102 cases. Indeed, although 100% of the infants survived after 10 yr (including 1 MNA out of 17), when the NB 4S was netrin-1 low, the 5-yr overall survival was only 46% when the NB 4S was netrin-1 high ($P = 0.0109$). Furthermore, 43% of the non-MNA patients with high-level netrin-1 expression died. More generally, when a similar overall survival analysis was performed on all infants with stage 4 NB (i.e. stage 4S and [1yr$^-$] stage 4), a similar dichotomy was observed. Indeed, 5-yr overall survival was found to be 90% for the netrin-1–low infants yet only 48% for netrin-1–high infants ($P = 0.032$; Fig. 1 F). These data suggest that netrin-1 is a potential prognostic marker for aggressiveness in stage 4 NB diagnosed in infants. Whether or not it constitutes an independent prognostic marker of stage 4 NB in neonates and infants deserves to be tested in a larger patient cohort. Nevertheless, these data indicate that a netrin-1 threshold may turn as an alternative determinant for the biological behavior of stage 4 NB in infants, potentially suggesting its involvement in a cell death process of very early childhood neuroblasts, reminiscent of that operating during nervous system development (31).

Netrin-1 high expression is not only detected in 38% of [1yr$^+$] stage 4 and in poor outcome [1yr$^-$] stage 4 primary NB tumors but also in a fraction of NB cell lines mainly derived from stage 4 tumor material (Fig. 2 A and Fig. S2 A). Two human NB cell lines, IMR32 (netrin-1 high) and CLB-Ge2 (netrin-1 low), were evaluated further. In spite of a marked difference in netrin-1 and DCC expression, the UNC5H levels

are similar in IMR32 and CLB-Ge2 cells: UNC5H1, UNC5H3, and UNC5H4 show the highest expression (Fig. 2 B). Specifically, UNC5H1, UNC5H3, and UNC5H4 proteins could be detected at the plasma membrane by confocal analysis (Fig. 2 C). To test the hypothesis that the high netrin-1 mRNA levels detected in IMR32 cells are associated with an autocrine netrin-1 production, we next performed netrin-1 immunohistochemistry on IMR32 and CLB-Ge2 cells. As shown in Fig. 2 D, a netrin-1–specific membrane staining was detected in a homogeneous pattern in IMR32 cells, whereas no specific staining was detected for CLB-Ge2 cells. Confocal analysis further confirmed the presence of netrin-1 at the cell membrane (Fig. 2 E

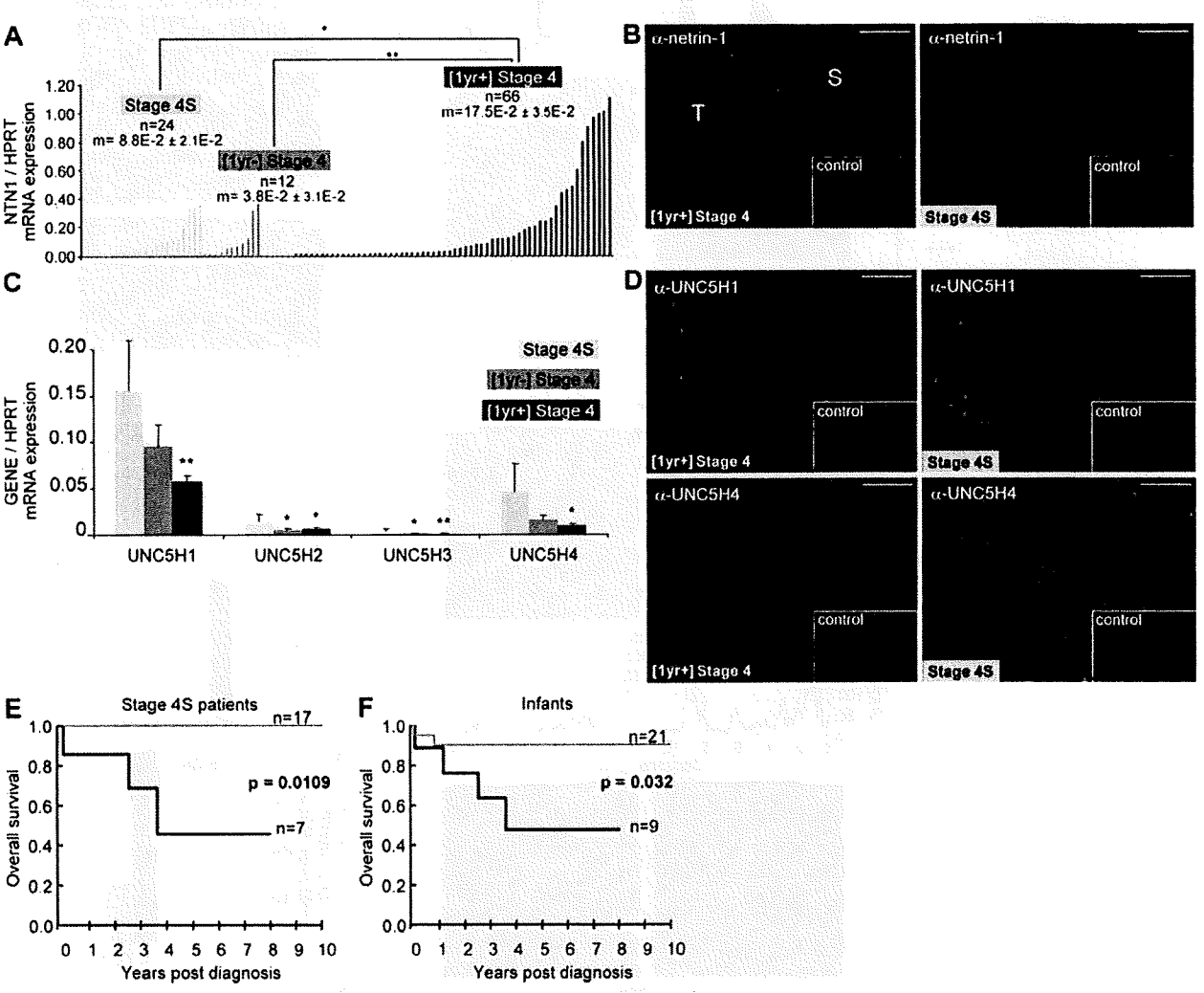

Figure 1. Netrin-1 up-regulation is detected in aggressive NB. (A) Netrin-1 mRNA levels in 102 stage 4S (n = 24), [1yr$^-$] stage 4 (n = 12), and [1yr$^+$] stage 4 (n = 66) NBs measured by Q-RT-PCR. HPRT housekeeping gene was used as a control. Mean netrin-1 mRNA expression value for each subgroup is indicated by an "m" value. Mean netrin-1 mRNA levels in stage 4S and [1yr$^-$] stage 4 were, respectively, compared with the mean netrin-1 detected in [1yr$^+$] stage 4. The data were statistically determined using Student's t test compared with levels of [1yr$^+$] stage 4. *, $P < 0.05$; **, $P < 0.01$. Each sample was assessed in two independent experiments. (B) Representative netrin-1 immunohistochemistry on one [1yr$^+$] stage 4 and one stage 4S tumor. Insets show control without primary antibody. Bars, 50 µm. T, tumor cells; S, stromal cells. Netrin-1 antibody specificity is further shown in Fig. 2 D and Fig. S1 B. Immunohistochemistry was performed on four [1yr$^+$] stage 4 and four stage 4S tumors. (C) Mean UNC5H mRNA levels in the different stage 4 NBs. Q-RT-PCR using UNC5H1–4-specific primers was performed. Mean UNC5H1–4 mRNA levels in [1yr$^-$] stage 4 and [1yr$^+$] stage 4 were, respectively, compared with the mean UNC5H1–4 levels detected in stage 4S. Error bars indicate SEM. The data were statistically determined using Student's t test compared with levels of stage 4S. *, $P < 0.05$; **, $P < 0.01$. Samples were analyzed in duplicates for each gene. (D) Representative UNC5H1 and UNC5H4 immunohistochemistries on [1yr$^+$] stage 4 and stage 4S tumors. Insets show control without primary antibody. Bars, 50 µm. Immunohistochemistry was performed on four stage 4 [1yr$^+$] and four stage 4S tumors. (E) Netrin-1 up-regulation is a marker of poor prognosis in stage 4S NB. Overall survival in a panel of 24 infants diagnosed with stage 4S NB with primary tumors showing either netrin-1–low (gray) or netrin-1–high (black) levels. The data was statistically determined using the Kaplan-Meier method. P-value is indicated. (F) Netrin-1 up-regulation is a marker of poor prognosis in infants with NB. Data are presented as in E, with a panel of 30 infants bearing NB.

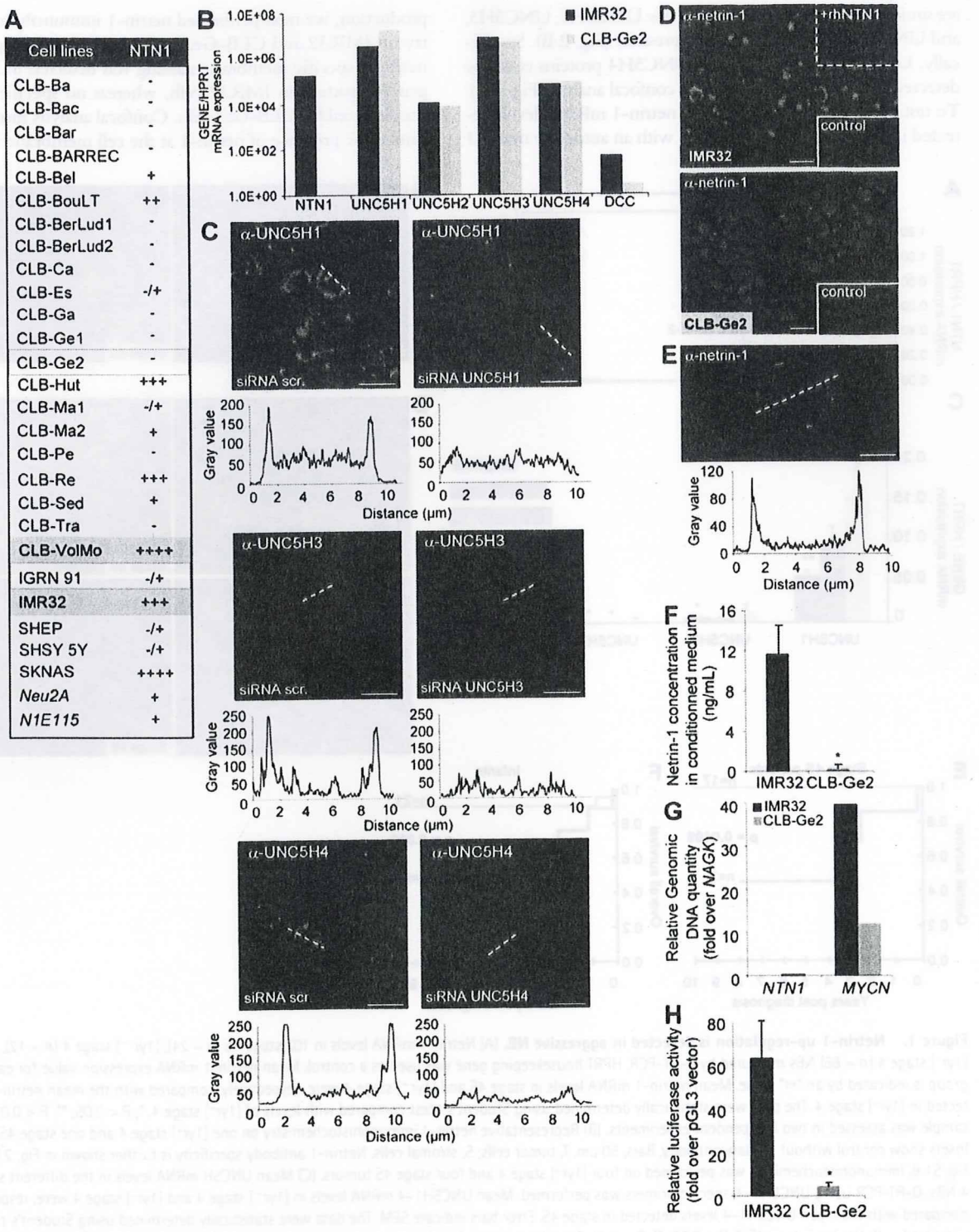

Figure 2. Netrin-1 up-regulation is detected in NB cell lines. (A) Netrin-1 expression measured by Q-RT-PCR in a panel of 28 NB cell lines. HPRT housekeeping gene was used as a control. The netrin-1 level is indicated as follows: −, not detectable; −/+, barely detectable; + to ++++, moderate to very high expression. Mouse cell lines are in italics. Cell lines outlined and highlighted in grey are, respectively, netrin-1–low and netrin-1–high cell lines further used in the experiments. (B) Netrin-1 receptor expression in IMR32 and CLB-Ge2 cell lines. DCC/UNC5H Q-RT-PCR was performed on netrin-1–expressing (IMR32) or netrin-1–low (CLB-Ge2) cells using specific primers. Ratio of netrin-1 and netrin-1 receptor expression to the HPRT housekeeping

and Fig. S2 B). To further analyze whether netrin-1 is secreted from IMR32 cells, netrin-1 ELISA assay was used to detect netrin-1 in the conditioned medium. As shown in Fig. 2 F, 11.7 ng/ml netrin-1 was recovered from the conditioned medium of IMR32 cells, whereas no netrin-1 was detected from the conditioned medium of CLB-Ge2 cells. Thus, together these data suggest that the high netrin-1 content observed in aggressive NB could result from an autocrine expression of netrin-1 in NB cells.

As a first approach to apprehend the mechanisms leading to netrin-1 up-regulation in aggressive NB, we analyzed whether netrin-1 gene (*NTN1*) is amplified in IMR32 cells. As shown in Fig. 2 G, although *MYCN* was amplified both in IMR32 and CLB-Ge2 cells compared with the *NAGK* control gene, the *NTN1* gene was not found to be amplified in these two cell lines. We then analyzed whether the increase in netrin-1 expression could be caused by a differential netrin-1 promoter activation. A luciferase reporter gene fused to netrin-1 promoter (32) was then transfected into IMR32 or CLB-Ge2 cells, and luciferase activity was reported to an internal control in each cell line. As shown in Fig. 2 H, netrin-1 promoter activity was 13.8-fold higher in IMR32 cells than in CLB-Ge2 cells, thus supporting the view that netrin-1 up-regulation in NB is related to a gain in netrin-1 promoter activation.

Netrin-1 up-regulation is a selective advantage for NB cell survival

To investigate whether the netrin-1 autocrine expression observed in IMR32 cells provides a selective advantage for survival, as would be expected from the dependence receptor theory, cell death was analyzed in response to the disruption of this autocrine loop. As a first approach, netrin-1 was down-regulated by RNA interference. As shown in Fig. 3 A, the addition of netrin-1 small interfering RNA (siRNA) to IMR32 cells was associated with a significant reduction in netrin-1 mRNA. This mRNA reduction was associated with a decrease of netrin-1 protein as observed by immunohistochemistry (Fig. 3 B). Although scramble siRNA failed to affect IMR32 cell survival, as measured by trypan blue exclusion, netrin-1 siRNA treatment was associated with IMR32 cell death (Fig. 3 C). In contrast, CLB-Ge2 cell survival was unaffected after netrin-1 siRNA treatment (Fig. 3 C). To determine whether this increase in cell death was in part caused by an increase in apoptotic cell death, caspase-3 activity was measured in response to netrin-1 siRNA treatment. As shown in Fig. 3 D, although significant apoptotic cell death was detected upon netrin-1 siRNA treatment in IMR32 cells, no such effect was observed in CLB-Ge2 cells. A similar proapoptotic effect of the netrin-1 siRNA was observed in CLB-VolMo cells, another netrin-1 high cell line (unpublished data).

Interference with netrin-1 triggers UNC5H-induced apoptosis in NB cells

As a second approach, we looked for a compound that could interfere with the netrin-1 ability to block DCC/UNC5H proapoptotic activity. We recently reported that the fifth fibronectin type III domain of DCC (DCC-5Fbn; Fig. 4 A), which is located in the DCC ectodomain, interacts with netrin-1 and blocks the ability of netrin-1 to trigger multimerization of DCC and UNC5H receptors. Because multimerization inhibits DCC or UNC5H-induced cell death (unpublished data), DCC-5Fbn antagonizes netrin-1 function, disrupting netrin-1–mediated inhibition of DCC/UNC5H proapoptotic activity. Thus, DCC-5Fbn acts as a trap for netrin-1 survival function. As shown in Fig. 4 (B–D), the addition of DCC-5Fbn, but not the unrelated protein IL3R, triggered IMR32 apoptotic cell death as measured by trypan blue exclusion (Fig. 4 B), caspase-3 activity assay (Fig. 4 C), and terminal deoxynucleotidyl transferase–mediated dUTP-biotin nick end labeling (TUNEL) staining (Fig. 4 D). This effect was specific for netrin-1 inhibition because DCC-5Fbn had no effect on CLB-Ge2 cells, and the addition of netrin-1 ultimately reversed the DCC-5Fbn–induced IMR32 apoptotic cell death (Fig. 4, B–D). Similar results were obtained with the CLB-VolMo cells (Fig. S2 D). To determine whether the ability of DCC-5Fbn to kill NB cells is restricted to established NB cell lines, a surgical biopsy from a tumor with high netrin-1 level (unpublished data) was semidissociated and further incubated with DCC-5Fbn. As shown in Fig. 4 E, DCC-5Fbn triggered cell death as measured by caspase-3 activation, demonstrating that in vitro, disruption of the netrin-1 autocrine loop is associated with NB cell death.

We next investigated whether netrin-1 autocrine expression in NB cells acts as a general cell survival factor, i.e., whether it has a trophic effect similar to that of neurotrophins, or whether it specifically inhibits death induced by

gene is presented. (C) Confocal analysis of UNC5H1, UNC5H3, and UNC5H4 receptor immunostaining in human IMR32 cells. Left and right correspond to IMR32 cells transfected with scramble siRNA and specific siRNA UNC5H, respectively. A fluorescence intensity profile corresponding to the white dashed bar is presented under each panel. Bars, 10 µm. (D) Immunostaining on human IMR32 and CLB-Ge2 cell lines using netrin-1 antibody. Bottom insets show control without primary antibody. Top inset: antibody specificity was tested by adding human recombinant netrin-1. Bars, 50 µm. (E) Confocal analysis of netrin-1 immunostaining on IMR32 cells. A fluorescence intensity profile corresponding to the white dashed bar is presented below. Bar, 5 µm. (F) Quantification of netrin-1 protein secreted in IMR32 and CLB-Ge2 cells conditioned medium by sandwich ELISA assay. Quantification in ng/ml was made according to a dose curve done with recombinant human netrin-1. Data are means of three independent experiments. Error bars indicate SEM. *, $P < 0.05$ using a two-sided Mann-Whitney test compared with level in IMR32 cells. (G) Quantification of *NTN1* and *MYCN* genomic DNA compared with control *NAGK* genomic DNA by PCR, using genomic DNA specific primers for each gene, in IMR32 and CLB-Ge2 cells. (H) Quantification of *NTN1* promoter activity in IMR32 and CLB-Ge2 cells. Both cell lines were transfected with the vector pGL3-NetP-Luc encoding luciferase under the control of *NTN1* promoter. Data presented are normalized on luciferase activity in cells transfected with pGL3 empty vector. Data are means of four independent experiments. Error bars indicate SEM. *, $P < 0.05$ using a two-sided Mann-Whitney test compared with levels in IMR32 cells.

netrin-1 dependence receptors. IMR32 cells were transfected with either a dominant-negative mutant for DCC (DN-DCC) or UNC5H (DN-UNC5H) proapoptotic activity. These dominant-negative mutants of dependence receptors actually encode the intracellular domain of these receptors mutated in their caspase cleavage sites, and these mutants have been shown both in vitro and in vivo to specifically block the proapoptotic activity of their wild-type counterparts (3, 9, 33). Cell death was then analyzed after netrin-1 inhibition by siRNA. Although DN-DCC expression failed to inhibit netrin-1 siRNA-induced IMR32 cell death, expression of DN-UNC5H rendered IMR32 cells resistant to netrin-1 siRNA (Fig. 5 A). To more formally exclude the role in this death process of DCC or of altered forms of DCC that are known to be expressed in IMR32 cells (Fig. S2 C) (34), DCC was down-regulated by a siRNA approach and cell death was induced via netrin-1 siRNA. As shown in Fig. 5 B, DCC siRNA had no effect on cell death per se and failed to inhibit netrin-1 siRNA-induced caspase-3 activation, strengthening the perception that in these cells DCC is not proapoptotic. Neogenin, a DCC homologue, has also been proposed to act as a receptor for netrin-1 (35, 36) even though this is still a matter of controversy (5, 37). We then investigated whether neogenin, which is expressed in IMR32 cells (Fig. S2 C), could be implicated in the IMR32 cell death observed here. Neogenin was down-regulated by a siRNA approach and, as shown in Fig. S3 A, this has no effect on netrin-1 siRNA-mediated IMR32 cell death. Thus, the netrin-1 autocrine loop probably blocks UNC5H-induced IMR32 cell death.

To more specifically address the identity of the UNC5H receptors involved in this cell death induction, we down-regulated the expression of each UNC5H receptor individually (UNC5H1, UNC5H2, UNC5H3, or UNC5H4) by a siRNA approach (Fig. 5 C and Fig. S3 B) while inducing cell death using netrin-1 siRNA (Fig. S3 C). None of the single UNC5H siRNAs was sufficient to inhibit netrin-1 siRNA-mediated IMR32 cell apoptosis, suggesting some redundancy in UNC5H-induced cell death (Fig. 5 D). However, when combinations of siRNAs were used, we observed that combined silencing of the four UNC5H receptors was sufficient to fully inhibit the death triggered by netrin-1 autocrine loop disruption (Fig. 5 D), whereas the same combination of siRNAs had no effect on CLB-Ge2 cell survival (Fig. S3 D). The respective importance of UNC5H receptors in netrin-1 siRNA-induced cell death was then assessed by the different combination of two or three siRNAs; the combination of UNC5H1, UNC5H3, and UNC5H4 siRNAs was the only one to fully block cell death (Fig. 5 E). Thus, in agreement with the level of UNC5H receptors expressed in IMR32 cells, it appears that disruption of the netrin-1 autocrine survival loop triggers UNC5H-induced cell death. Moreover,

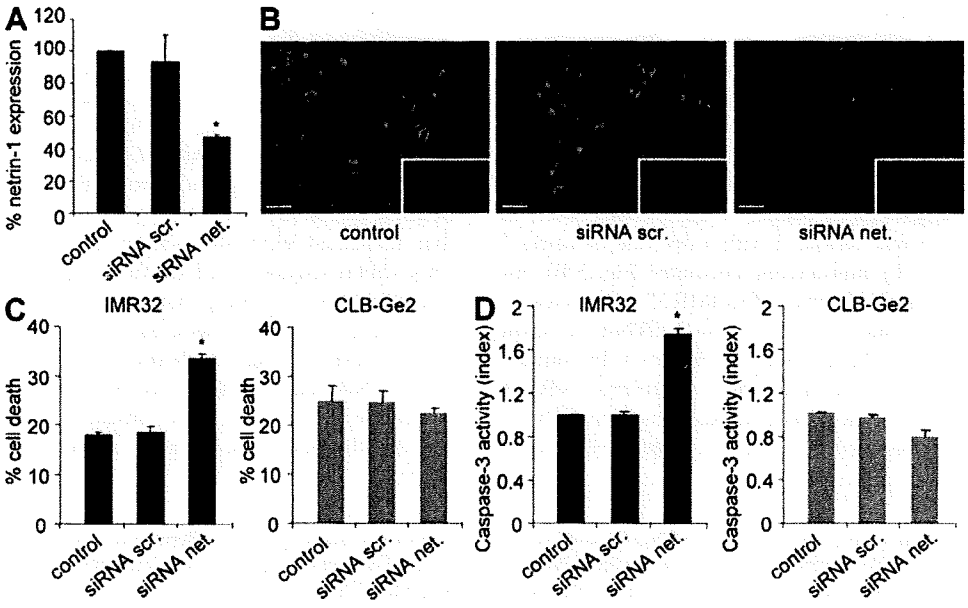

Figure 3. Down-regulation of netrin-1 autocrine loop by siRNA triggers NB tumor cell death. (A) Analysis of netrin-1 expression using Q-RT-PCR in nontransfected (control) IMR32 cell line or 24 h after transfection with scramble siRNA (siRNA scr.) or with netrin-1 siRNA (siRNA net.). Data are means of three independent experiments. Error bars indicate SEM. *, $P < 0.05$ using a two-sided Mann-Whitney test compared with levels in control. (B) Immunostaining on IMR32 cell line using netrin-1 antibody in the absence of transfection (control) or 24 h after transfection with scramble siRNA or netrin-1 siRNA. Note that the general caspase inhibitor z-VAD-fmk was added to avoid cell death induced by netrin-1 siRNA. Insets show control without primary antibody. Bars, 50 μm. (C and D) Cell death induction in IMR32 and CLB-Ge2 cell lines was quantified in nontransfected cells (control) or after transfection with either scramble siRNA or netrin-1 siRNA using trypan blue exclusion assay (C) or relative caspase-3 activity assay (D). Data are means of four independent experiments. In C and D, error bars indicate SEM. *, $P < 0.05$ calculated using a two-sided Mann-Whitney test compared with level of control.

UNC5H1, UNC5H3, and UNC5H4 are the receptors involved in this proapoptotic effect.

Furthermore, in IMR32 cells, the proapoptotic serine threonine kinase DAP kinase (DAPK), which is shown to be required for UNC5H-induced cell death, exhibited a loss of its inhibitory autophosphorylation (38) upon DCC-5Fbn treatment (Fig. 5 F) or netrin-1 siRNA transfection (Fig. 5 G). Accordingly, autophosphorylation was restored by a treatment with excess netrin-1 or by a combination of UNC5H1, UNC5H3, and UNC5H4 siRNAs. Moreover, the transfection of the antiapoptotic protein BCL-2 was sufficient to inhibit netrin-1 siRNA-induced cell death but did not inhibit DAPK dephosphorylation, hence suggesting that DAPK activation is not a result of cell death but is specifically engaged by UNC5H after netrin-1 inhibition (unpublished data).

Interference with netrin-1 inhibits NB progression and dissemination

We next assessed whether in vivo modulation of netrin-1 could be used to limit/inhibit NB progression and dissemination. An elegant chicken model has been developed in which graft of NB cells in the chorioallantoic membrane (CAM) of 10-d-old chick embryos recapitulates both tumor growth at a primary site, i.e., within the CAM, and tumor invasion and dissemination at a secondary site, metastasis to the lung (Fig. 6 A). In a first approach, IMR32 or CLB-Ge2 cells were loaded in

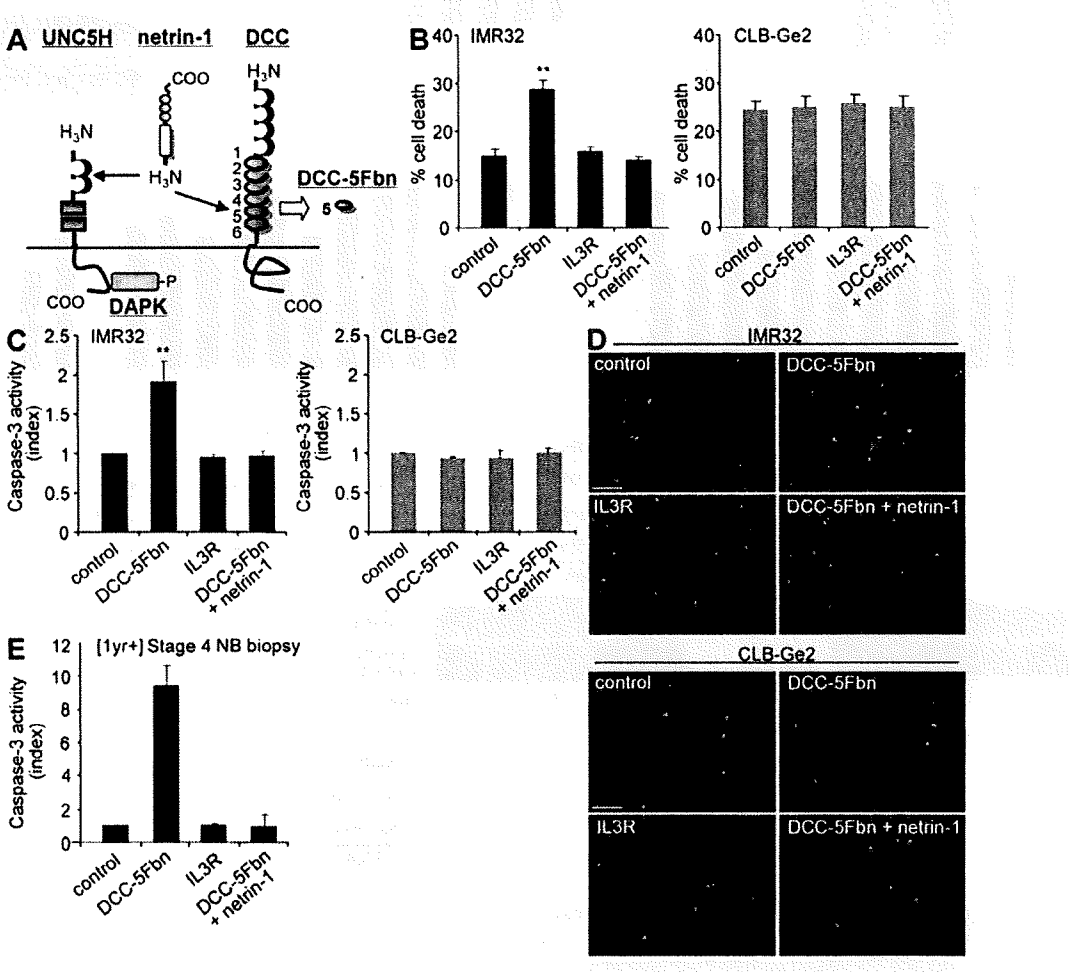

Figure 4. Disruption of netrin-1 autocrine loop by a decoy receptor fragment triggers NB tumor cell death. (A) Scheme representing netrin-1 and its receptors DCC and UNC5H and the fifth fibronectin type III domain of DCC (DCC-5Fbn) used to induce cell death. The downstream effector DAPK implicated in UNC5H-induced cell death is also represented. (B–D) Quantitative analysis of cell death in IMR32 and CLB-Ge2 cell lines treated with 1 µg/ml DCC-5Fbn, with or without addition of netrin-1 in excess (150 ng/ml) to reverse the effect of DCC-5Fbn. A negative control was also performed by adding an unrelated IL3R peptide produced in the same condition as DCC-5Fbn. Cell death was quantified by trypan blue exclusion assay (B) while apoptosis was monitored by measuring relative caspase-3 activity (C) or by TUNEL staining (D). Bars, 100 µm. In D, TUNEL staining was performed on three independent experiments. (E) Effect of DCC-5Fbn on fresh [1yr+] stage 4 NB. Tumoral cells were directly resuspended from the surgical punction and were plated for 24 h in presence of treatment. In B and C, data are means of six independent experiments. In E, data are means of two independent experiments. Error bars indicate SEM. **, $P < 0.01$ calculated using a two-sided Mann-Whitney test compared with level of control.

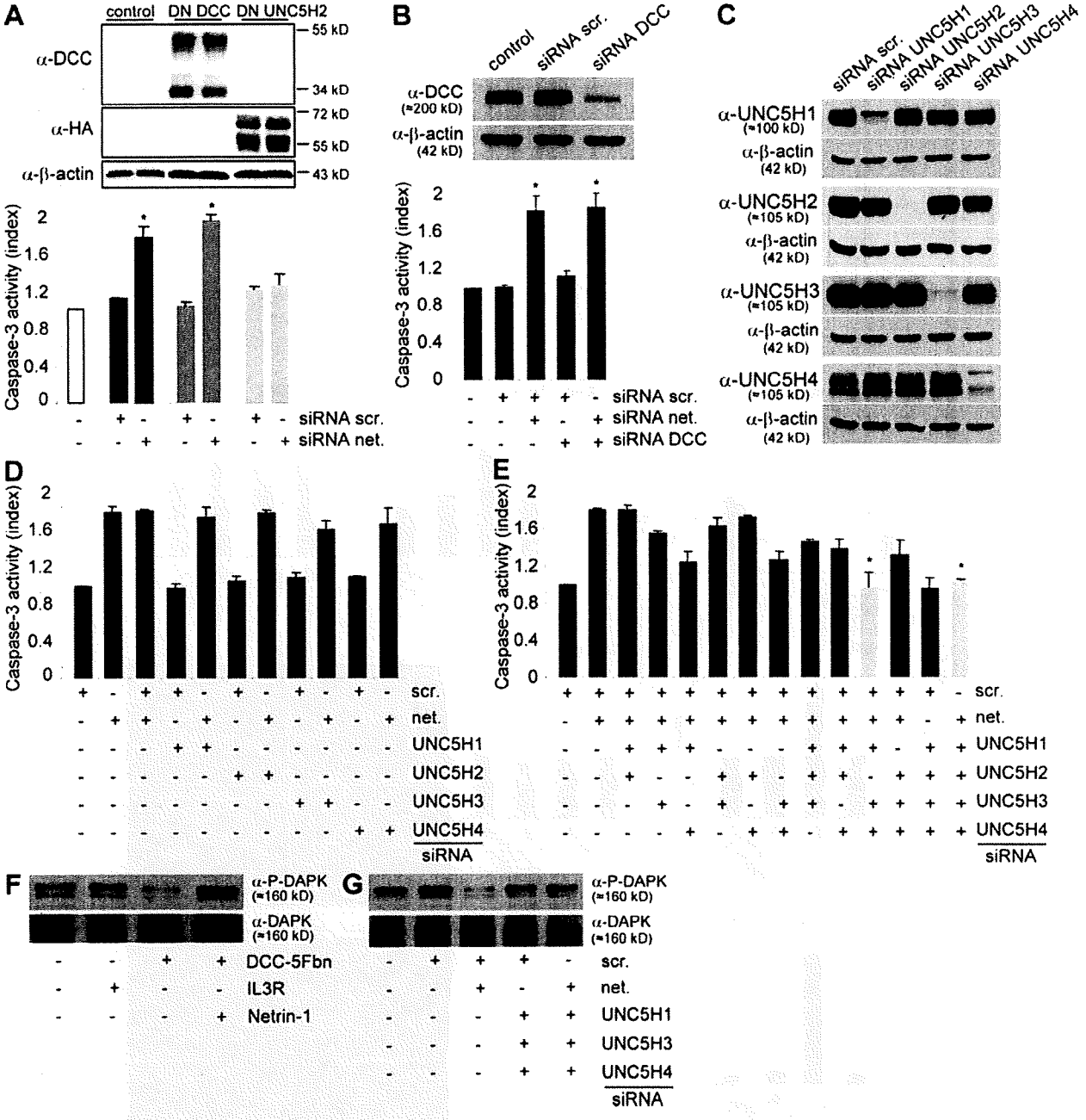

Figure 5. NB tumor cell death occurs via UNC5H/DAPK proapoptotic signaling. (A) Quantification of cell death in IMR32 cells transfected with either a dominant-negative mutant for DCC proapoptotic activity (DN-DCC) or a dominant-negative mutant for UNC5H proapoptotic activity (DN-UNC5H). Top: DN-DCC and DN-UNC5H proteins expression were analyzed by Western blot. Bottom: cell death was quantified by measuring relative caspase-3 activity after scramble or netrin-1 siRNA transfection. SEM are indicated. Data are means of three independent experiments. *, $P < 0.05$ calculated using a two-sided Mann-Whitney test compared with level of control. (B) Quantification of cell death in IMR32 cells transfected with either a scramble siRNA or a netrin-1 siRNA together or not with a DCC siRNA. Top: DCC siRNA efficiency was verified by Western blotting on HEK293T cells transfected with pCR-hDCC together with scramble or DCC siRNA. Bottom: cell death was quantified by measuring relative caspase-3 activity. Data are means of three independent experiments. SEM are indicated. *, $P < 0.05$ calculated using a two-sided Mann-Whitney test compared with level of control. Similar results were obtained when neogenin or MYCN were down-regulated (Fig. S3 A). (C) Analysis of specificity and efficiency of each UNC5H siRNA by Western blot in HEK293T cells transfected with UNC5H1, H2, H3, or H4 encoding vector together with each UNC5H siRNA. (D and E) Quantification of cell death in IMR32 cells transfected with either a scramble siRNA or a netrin-1 siRNA together with various combinations of UNC5H siRNA, i.e, one UNC5H (D) or two or four UNC5H (E). Apoptosis was monitored by measuring relative caspase-3 activity. The use of combined UNC5H1, UNC5H2, UNC5H3, and

10-d-old CAM and embryos were treated on days 11 and 14 with PBS or DCC-5Fbn. 17-d-old chicks were then analyzed for primary tumor growth and metastasis to the lung. As shown in Fig. 6 (B and C), specifically in CAMs grafted with IMR32 but not with CLB-Ge2 cells, DCC-5Fbn significantly reduced primary tumor size. This size reduction was associated with increased tumor apoptosis, as shown by an increased caspase-3 activity in the tumor lysate (Fig. 6 D). More importantly, DCC-5Fbn also reduced lung metastasis formation, as shown in Fig. 6 E. Similar results were obtained when CAM-grafted embryos were treated with netrin-1 siRNA (unpublished data). To next assess whether DCC-5Fbn could also induce the regression of metastatic lesions, IMR32 cells were CAM grafted and DCC-5Fbn (or PBS) treatment started after metastasis to the lung is known to occur, i.e., treatments were performed on days 14 and 15 because pulmonary metastases are routinely detectable at day 13. As shown in Fig. 6 F, pulmonary metastases were markedly reduced, suggesting that DCC-5Fbn not only inhibits tumor dissemination but also induces regression of metastatic lesions at the secondary site.

As a second in vivo approach, we used the IGR-N-91 model derived from a BM metastasis of human MYCN-amplified stage 4 NB. When subcutaneously xenografted into nude mice, IGR-N-91 cells gave rise to different tumor cell lines derived from the *nude* mouse primary tumor xenograft (PTX) or from disseminated metastatic foci into BM, blood, and myocardium (Myoc) of the animal (39). It is of interest that although the parental IGR-N-91 and the cell line derived from the PTX show no or very low netrin-1 expression, the different cell lines derived from secondary localizations showed a marked expression of netrin-1 both at the RNA level (Fig. 7 A) and at the protein level (Fig. 7 B). When cell death was investigated in these different cell lines upon treatment with DCC-5Fbn, a direct correlation was observed between the level of netrin-1 and cell susceptibility to DCC-5Fbn (Fig. 7 C). Specifically, although PTX cells failed to undergo cell death upon DCC-5Fbn treatment, this treatment triggered netrin-1–high Myoc cell death (Fig. 7 C). This observation supports the overall view that gaining netrin-1 dependence receptor resistance, via an autocrine netrin-1 expression in the case of the IGR-N-91 model, likely promotes NB tumor cell survival outside of the primary tumor site. To test whether this netrin-1 expression may then be used as a target to inhibit metastasis in vivo, Myoc and PTX cells were injected intravenously into *nude* mice and lung colonization was quantitated after daily intraperitoneal treatment with PBS or DCC-5Fbn. Although lung colonization was not reduced upon DCC-5Fbn treatment in PTX-injected mice (not depicted), a significant decrease in lung colonization was detected in DCC-5Fbn–treated Myoc-injected mice (Fig. 7 D). Thus, in both chick and mouse models, disruption of the netrin-1 autocrine loop inhibited or completely prevented the dissemination of netrin-1–expressing NB cells.

DISCUSSION

Together, the data obtained in the chick and mouse models described in the previous sections, in NB cell lines, and in the human pathology all support the view that a fraction of NB shows an autocrine production of netrin-1. This elevated netrin-1 level likely confers a selective advantage acquired by the cancer cell to escape netrin-1 dependence receptor–induced apoptosis and, consequently, to survive in settings of environmental absence or limitation of netrin-1. It is therefore interesting to note that not only NB but also other neoplasms associated with poor prognosis, for example, metastatic breast cancer and pancreatic cancer, also express high levels of netrin-1 (33, 40), suggesting that netrin-1 up-regulation may be a common feature for several aggressive cancers. From a mechanistic point of view, in a large fraction of NB, this autocrine expression of netrin-1 probably inhibits UNC5H-induced cell death. However, because DCC has been shown to display reduced expression in NB and because this reduction has been associated with NB aggressiveness in human NB (29), it is tempting to speculate that netrin-1 up-regulation can also, in some NB, inhibit DCC-induced apoptosis. Interestingly, this netrin-1 up-regulation appears to block a death signal involving the serine threonine DAPK, whose activity is regulated via its autophosphorylation. It is therefore of interest to note that DAPK was described to be a negative regulator of tumor progression and, more specifically, of metastasis (41). Thus, it can be suggested that a fraction of low netrin-1–expressing NB may have selected a loss of function of DAPK for survival. This would be compatible with the finding that metastasis in NB is associated with a loss of caspase-8, a selective advantage which provides survival to NB cells by inhibiting the proapoptotic signaling of the dependence receptor integrin $\alpha 3\beta 1$ (42).

It is then interesting to wonder why such a large fraction of aggressive NBs have selected a gain of netrin-1 rather than a loss of the netrin-1 dependence receptor death pathways. A possible explanation is that netrin-1 expression not only confers a gain in survival, but may also lead to enhancement of non-apoptotic signaling mediated by netrin-1 receptors. Netrin-1 was indeed shown to bind a complex that includes some integrins (43). These integrins regulate cell migration and invasiveness and, thus, may play a role in cancer progression. Netrin-1 was also proposed to play a role in angiogenesis, although whether netrin-1 is proangiogenic or antiangiogenic is controversial (44–47) and this effect on angiogenesis may increase NB metastases development. It is also of interest to note that NB is a complex disease that originates from migrating neural crest cells. Netrin-1 up-regulation may then be implicated in

UNC5H4 or UNC5H1, UNC5H3, and UNC5H4 siRNAs, leading to the absence of death induced by netrin-1 siRNA, are presented in gray. Data are means of three independent experiments. Error bars indicate SEM. *, $P < 0.05$ calculated using a two-sided Mann-Whitney test compared with level of control. (F and G) Immunodetection of phosphorylated DAPK (P-DAPK) in IMR32 cells either treated with DCC-5Fbn (F) or transfected with netrin-1 siRNA alone or with UNC5H1, H3, and H4 siRNAs (G). In F and G, immunodetection was performed on three independent experiments.

the main function played by netrin-1 during nervous system development that is neuronal navigation. Along this line, netrin-1 and DCC have been shown to play an important role during neural crest cell migration (48), and it is then tempting to suggest that the gain in netrin-1 expression also promotes NB cell migration.

As different types of stage 4 NBs are distinguished, not only by the age of the children but also by the tissues in which metastases are found, one may wonder about the implication of netrin-1 produced in the normal tissues in which the tumor cells spread, and this would be interesting to explore. In particular, it would be interesting to evaluate whether, according to the classical "seed and soil" theory for metastasis (for review see reference 18), netrin-1 expression in specific tissues may favor metastasis development more specifically in these tissues. It is also intriguing

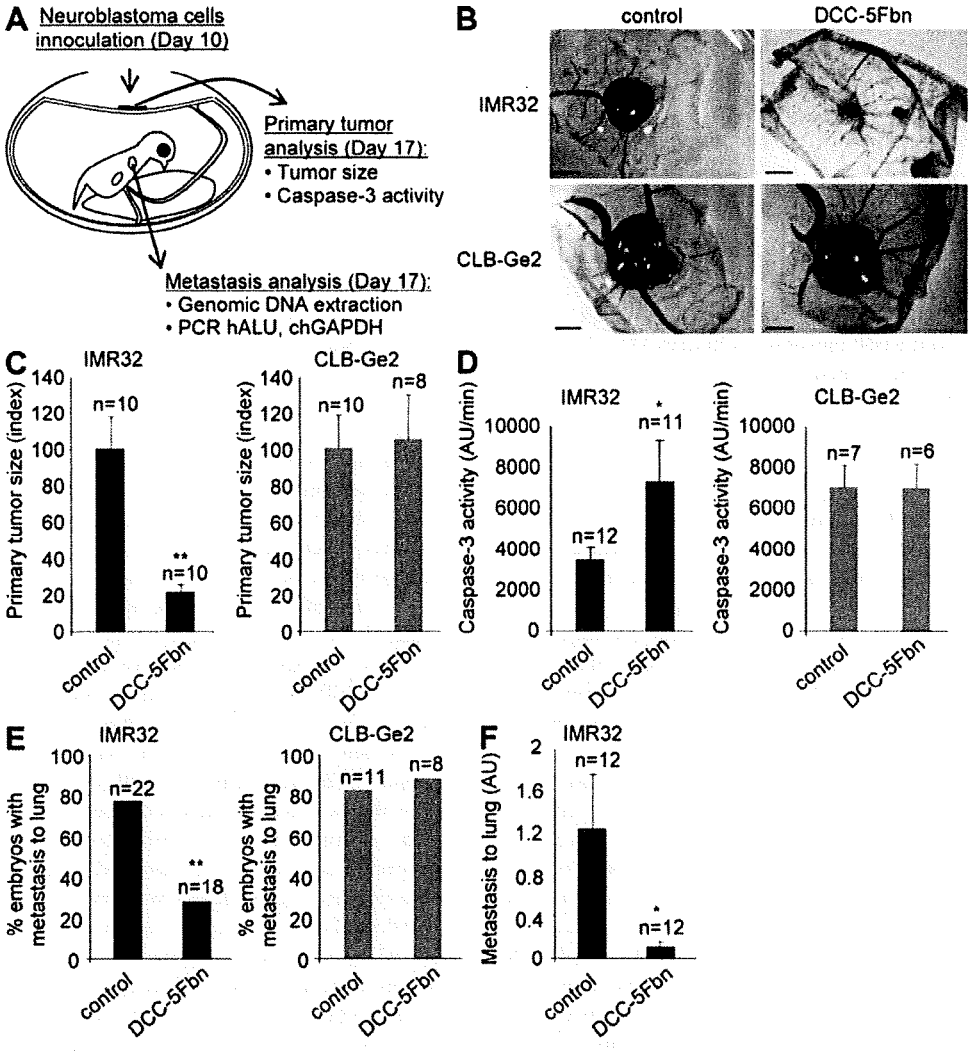

Figure 6. Disruption of netrin-1 autocrine loop inhibits NB progression and dissemination in a chick model. (A) Schematic representation of the experimental chick model. IMR32 or CLB-Ge2 cells were grafted in CAM at day 10 and DCC-5Fbn or PBS was injected on days 11 and 14. Tumors and lungs were harvested on day 17. (B–D) Effect of DCC-5Fbn on primary tumor growth and apoptosis. (B) Representative images of IMR32 (top) or CLB-Ge2 (bottom) primary tumors formed on CAM treated either with DCC-5Fbn (right) or PBS (left). Bars, 2 mm. (C) Quantitative analysis showing the mean primary tumor size. (D) Caspase-3 activity was determined in the primary tumor lysates from DCC-5Fbn/PBS-treated IMR32 or CLB-Ge2–grafted embryos. (E) Effect of DCC-5Fbn on lung metastasis. Percentage of embryos with lungs invaded by human IMR32 or CLB-Ge2 cells after two injections (days 11 and 14) of either DCC-5Fbn or PBS was performed as described in the Materials and methods. (F) Effect of DCC-5Fbn on lung metastasis regression. Quantification of lung metastasis in embryos CAM grafted with IMR32 cells and treated after metastasis formation (days 14 and 15) with DCC-5Fn or PBS. The number of embryos studied in each condition is indicated above the graphs and results are from three independent experiments. In C–F, errors bars indicate SEM. C–F: *, $P < 0.05$; **, $P < 0.005$ calculated using a two-sided Mann-Whitney test compared with level of control. E: **, $P < 0.005$ calculated using a Chi-squared test.

to note that others have shown that in some particular cell lines, netrin-1 is able to promote apoptosis rather than inhibit apoptosis (49), so that the view of netrin-1 up-regulation being only a survival-selective advantage to block apoptosis via dependence receptors is probably only part of the overall regulatory mechanisms that links NB, netrin-1, and its receptors.

The observation that low levels of netrin-1 in NB correlate with good outcome is of clinical interest, in particular in NB diagnosed in neonates and infants. Indeed, low netrin-1 expression predicts long-term survival in infants (100% in 4S stage and 90% in infants in general) in a type of pathology in which therapeutic management is highly dependent on presentation and MNA (50, 51). This is particularly true with

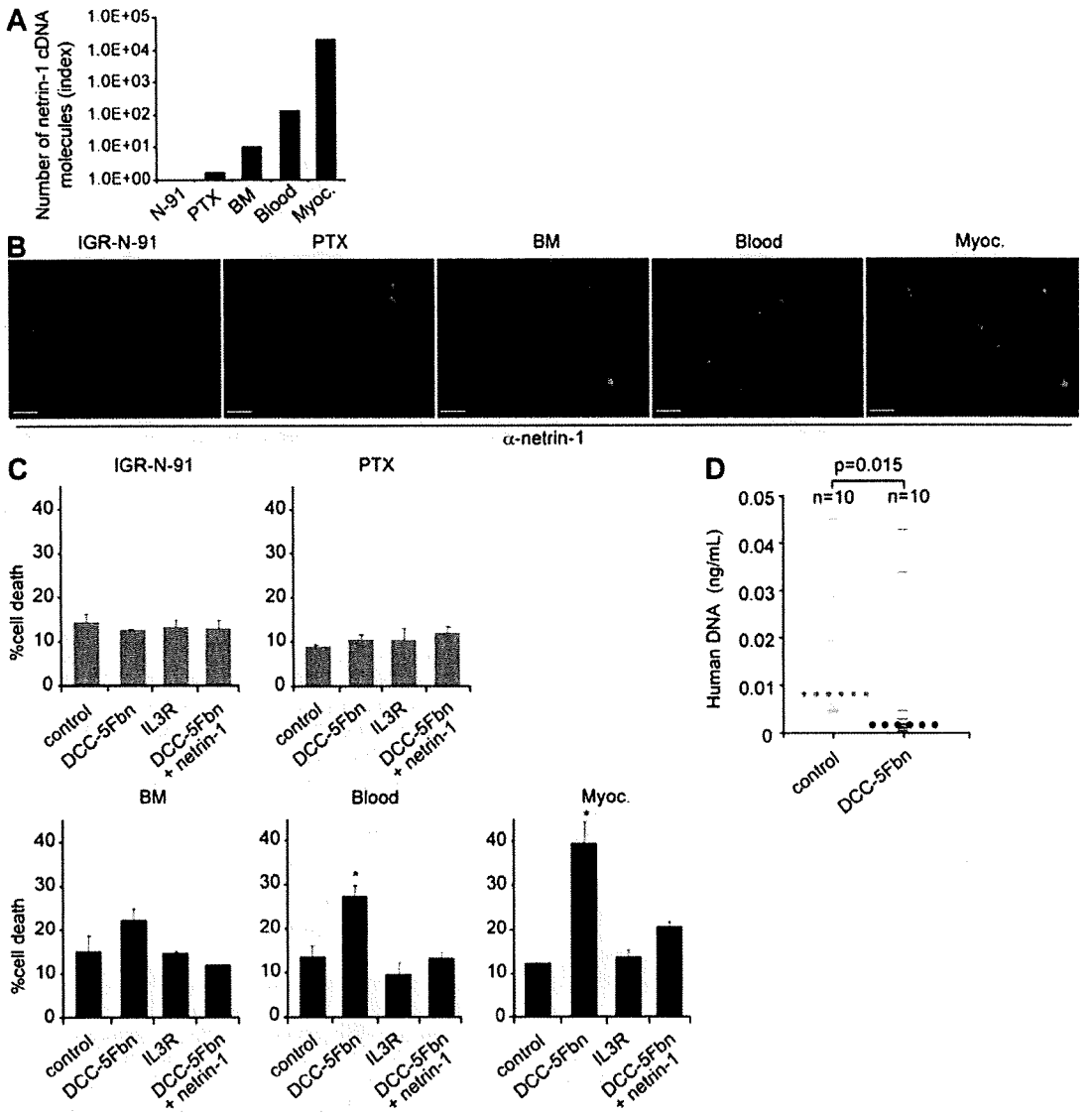

Figure 7. Disruption of netrin-1 autocrine loop inhibits NB dissemination in a mouse model. (A) Analysis of netrin-1 expression using Q-RT-PCR in IGR-N-91 cell line and the IGR-N-91–derived cell lines PTX, BM, Blood, and Myoc. Note that although PTX cells fail to express netrin-1, netrin-1 mRNA is highly expressed in Myoc cells. (B) Immunostaining on IGR-N-91 cells and the different derived cell lines PTX, BM, Blood, or Myoc using netrin-1 antibody. Bar, 50 µm. (C) Cell death was quantified in IGR-N-91, PTX, BM, Blood, or Myoc cell lines treated or not with DCC-5Fbn, with or without addition of netrin-1 in excess to reverse the effect of DCC-5Fbn. A negative control was also performed by adding an unrelated IL3R peptide produced in the same condition as DCC-5Fbn. Data are means of three independent experiments. Errors bars indicate SEM. *, $P < 0.05$, calculated using a two-sided Mann-Whitney test compared with level of control. (D) Quantification of lung colonization in PTX or Myoc cells in i.v injected mice treated with PBS or DCC-5Fbn for 22 d. Quantification was performed as described in the Materials and methods. Large bars indicate the median values for both groups. P-value was calculated using a two-sided Mann-Whitney test compared with level of control.

stage 4S infants who receive no (or minimal) treatment based on the lack of MNA, even though current statistics show that 1 in 10 of these infants will eventually die of NB. In this paper, we propose that determination of low netrin-1 level confirms a good prognosis for these infants without therapy, whereas the infants with high netrin-1 expression should be considered for more intensive treatment. Regarding infants or children with high netrin-1–expressing NB tumors, an alternative or supplementary targeted treatment based on disruption of the netrin-1 autocrine survival loop may improve standard high-dose chemotherapy regimen efficiency. We propose that a treatment based on inhibition of the interaction between netrin-1 and its dependence receptors, or inhibition of the ability of netrin-1 to multimerize its receptors, could potentially improve the survival of a large fraction of the patients suffering from aggressive NB. Moreover, it is interesting to note that no correlation between netrin-1 up-regulation and molecular signature of apoptosis and invasion was observed in NB tumors (Fig. S1 D), strengthening the case for netrin-1 as an original target for NB. Future preclinical and clinical studies should assess whether such therapeutic strategies, which could include small molecules (drugs), monoclonal antibodies, or the DCC-5Fbn recombinant protein presented in this paper, used alone or in combination with standard chemotherapy, could be of therapeutic benefit for infants and children with NB.

MATERIALS AND METHODS

Cell lines, transfection procedure, and reagents. Human NB cell lines were obtained from the tumor banks at Centre Léon Bérard and at Institut Gustave Roussy. More specifically, IMR32 and CLB-Ge2 cell lines were cultured in RPMI 1640 GlutaMAX medium (Invitrogen) containing 10% FBS. IGR-N-91 cell line and its derivatives, as well as HEK293T cells, were cultured in DME medium (Invitrogen) containing 10% FBS. Cell lines were transfected using Lipofectamine 2000 reagent (Invitrogen) for siRNA or Lipofectamine Plus reagent (Invitrogen) for plasmids. Netrin-1 was obtained from Axxora and was used at a concentration of 150 ng/ml in all in vitro assays.

Human NB tumor samples and biological annotations. According to parental consent, surgical human NB tumor material was immediately frozen. Material and annotations were obtained from the Biological Resources Centers of both national referent Institutions for NB treatment (Centre Léon Bérard and at Institut Gustave Roussy). Protocols using human material were approved by the local ethics Committees of Lyon University and Paris XI University. MYCN genomic content was assessed on histologically qualified tumors as previously described (52). For immunohistochemistries, 5-µm sections were prepared and frozen at −80°C.

Plasmid constructs, siRNA, and DCC-5Fbn production. The dominant-negative mutant for UNC5H and DCC (pCR-UNC5H2-IC-D412N and pCR-DCC-IC-D1290N, respectively) and the plasmids encoding Neogenin (pCDNA3-Neogenin) and UNC5H1 (pCDNA3.1-UNC5H1-HA) have been previously described (1, 2, 5). The plasmids encoding UNC5H2 (pCDNA3.1-UNC5B-HA), UNC5H3 (pCDNA3-UNC5C-HA), and UNC5H4 (pCAG3-hU5H4-His) were gifts from H. Arakawa (National Cancer Institute, Tokyo, Japan), M. Tessier-Lavigne (Genentech, San Francisco, CA), K.L. Guan (University of Michigan, Ann Arbor, MI), and N. Yamamoto (Osaka University, Osaka, Japan). Human netrin-1–encoding plasmid (peak8-hNTN1-His) was obtained from D.E. Bredesen (The Buck Institute for Age Research, Novato, CA). Ps974-DCC-5Fbn allowing bacterial expression of the fifth fibronectin type III domain of DCC was obtained by inserting a PstI–BamHI DNA fragment generated by PCR using pDCC-CMV-S as a template. DCC-5Fbn production was performed using a standard procedure. In brief, BL21 cells were forced to express DCC-5Fbn in response to imidazole, and the BL21 lysate was subjected to affinity chromatography using FLAG-Sepharose (Sigma-Aldrich). A peptide corresponding to the ectodomain of IL3R was produced in the same conditions and used as a control. For cell culture use, netrin-1, DCC, and neogenin siRNAs (Santa Cruz Biotechnology, Inc.) were designed as a pool of three target-specific 20–25-nt siRNAs. UNC5H1, UNC5H2, UNCH3, and UNC5H4 siRNAs were designed by Sigma-Aldrich. MYCN siRNA was designed by Thermo Fisher Scientific.

Cell death assays. 2×10^5 cells were grown in serum-poor medium and were treated (or not) with 1 µg/ml DCC-5Fbn or transfected with siRNA using Lipofectamine 2000. Cell death was analyzed using trypan blue staining procedures as previously described (1). The extent of cell death is presented as the percentage of trypan blue–positive cells in the different cell populations. Apoptosis was monitored by measuring caspase-3 activity as described previously (1) using the Caspase 3/CPP32 Fluorimetric Assay kit (Gentaur). For detection of DNA fragmentation, treated cells were cytospun, and TUNEL was performed with 300 U/ml TUNEL enzyme and 6 µM biotinylated dUTP (Roche) as previously described (53).

Q-RT-PCR. To assay netrin-1, DCC, and UNC5H receptor expression in NB samples, total RNA was extracted from histologically qualified tumor biopsies (>60% immature neuroblasts) using the NucleoSpin RNAII kit (Macherey-Nagel), and 200 ng were reverse transcribed using 1U Superscript II reverse transcription (Invitrogen), 1U RNase inhibitor (Roche), and 250 ng of random hexamer (Roche). Total RNA was extracted from mouse and human cell lines using the NucleoSpin RNAII kit and 1 µg was reverse transcribed using the iScript cDNA Synthesis kit (Bio-Rad Laboratories). Real-time Q-RT-PCR was performed on a LightCycler 2.0 apparatus (Roche) using the LightCycler FastStart DNA Master SYBER Green I kit (Roche). Reaction conditions for all optimal amplifications, as well as primer selection for murine and human netrin-1, DCC, and UNC5H1-4, were determined as already described. The ubiquitously expressed human HPRT genes showing the least variability in expression in NB was used as an internal control (54). The sequences of the primers are the following: NTN1, 5′-TGCAAGAAGGACTATGCCGTC-3′ and 5′-GCTCGTGCCCTGCTTATACAC-3′; UNC5H1, 5′-CATCACCAAGGACACAAGGTTTGC-3′ and 5′-GGCTGGAAATTATCTTCTGCCGAA-3′; UNC5H2, 5′-GGGCTGGAGGATTACTGGTG-3′ and 5′-TGCAGGAGAACCTCATGGTC-3′; UNC5H3, 5′-GCAAATTGCTGGCTAAATATCAGGAA-3′ and 5′-GCTCCACTGTGTTCAGGCTAAATCTT-3′; UNC5H4, 5′-GGTGAACCCAGCCTCCAGTCAG-3′ and 5′-CTTCCACTGACATCACTTCCTCCC-3′; DCC, 5′-AGCCAATGGGAAAATTACTGCTTAC-3′ and 5′-AGGTTGAGATCCATGATTTGATGAG-3′; and HPRT, 5′-TGACACTGGCAAAACAATGCA-3′ and 5′-GGTCCTTTTCACCAGCAAGCT-3′.

Genomic DNA quantification. Genomic DNA from IMR32 and CLB-Ge2 cells was extracted with the NucleoSpin Tissue kit (Macherey-Nagel). 50 ng of genomic DNA was used to perform quantitative PCR using primers specific to *NTN1* and *MYCN* genomic sequences. Real-time quantitative PCR was performed on a LightCycler 2.0 apparatus using the Light Cycler FastStart DNA Master SYBER Green I kit. *NAGK* (the *N*-acetylglucosamine kinase gene), which is located on chromosome 2 similarly to the *MYCN* gene but separated from the MYCN amplicon, was used as an internal control gene to determine the gene dosage (55). For each pair of primers, genomic DNA amplification was assessed by polymerase activation at 95°C for 10 min, followed by 35 cycles at 95°C for 10 s, 65°C for 30 s, and 72°C for 10 s. The sequences of the primers are the following: *NTN1*, 5′-CTGTGTCCCCCACTTGTTCT-3′ and 5′-CCATGAACCCCACTGACTCT-3′; *MYCN*, 5′-GTGCTCTCCAATTCTCGCCT-3′ and 5′-GATGGCCTAGAGGAGGGCT-3′; and *NAGK*, 5′-TGGGCAGACACATCGTAGCA-3′ and 5′-CACCTTCACTCCCCACCTCAAC-3′.

Immunohistochemistry and immunoblotting analysis. 10^5 cells were centrifugated on coverslips with a cytospinner (Shandon Cytospin 3; Thermo Fisher Scientific). Tumor slides and cells were fixed in 4% paraformaldehyde. The slides were then incubated at room temperature for 1 h with an antibody recognizing the human netrin-1 (1:150; R&D Systems), UNC5H1 (1:100; Abcam), UNC5H3 (1:100; R&D system), or UNC5H4 (1:100; Santa Cruz Biotechnology, Inc.). After rinsing in PBS, the slides were incubated with an Alexa 488 donkey anti–rat antibody (Invitrogen), an Alexa 488 donkey anti–rabbit antibody (Invitrogen), a Cy3 donkey anti–mouse antibody (Jackson ImmunoResearch Laboratories), or an Alexa 488 donkey anti–goat antibody (Invitrogen), respectively. For tumor slides, netrin-1 and UNC5H4 signals were amplified using biotinyl-tyramide (TSA; Thermo Fisher Scientific) and Alexa 488–streptavidin (Invitrogen). Nuclei were visualized with Hoechst staining. Densitometric value corresponding to netrin-1 signal was quantified with AxioVision Release 4.6 software. Immunoblots were performed as already described using anti–phospho-DAPK and anti-DAPK (Sigma-Aldrich) (38), anti-DCC (1:500; Santa Cruz Biotechnology, Inc.), anti-neogenin (1:500; Santa Cruz Biotechnology, Inc.), anti-HA (1:7,500; Sigma-Aldrich), anti-HIS (1:1,000; QIAGEN), anti-MYCN (1:1000; BD), or anti-β-actin (1:1,000; Millipore) antibodies.

Netrin-1 ELISA assay. Detection of netrin-1 protein in IMR32 and CLB-Ge2 cell culture medium was performed using a modified ELISA assay. In brief, 96-well plates (Nunc-Immuno plate MaxiSorp; Thermo Fisher Scientific) were coated with 200 ng/well of purified recombinant extracellular domain of DCC (DCC-Ec-Fc). To minimize aspecific binding, each well was incubated with 100 µl of blocking solution, containing 5% (wt/vol) BSA (Sigma-Aldrich) in 0.05% PBS-Tween. 3 ml FBS free cell culture medium was added sequentially (300 µl/well) to coated 96-well plates and incubated for 1 h at 37°C. After three washes with 0.5% BSA PBS, 100 µl of rat anti–netrin-1 antibody (diluted 1:500 in blocking solution) was added to each well and incubated for 30 min at 37°C. After extensive washing, each well was incubated with 100 µl HRP-conjugated goat anti–rat antibody (1:1,000; Jackson ImmunoResearch Laboratories) for 30 min at 37°C. After removal of unbound antibody by three washes in 0.5% BSA/PBS, the plates were incubated for 5 min at room temperature with ECL Western Blotting Substrate (Thermo Fisher Scientific). Luminescent signal was measured using a Luminoskan Ascent apparatus (Thermo Fisher Scientific).

Reporter assay. 10^5 cells were plated in 12-well plates and transfected with the firefly luciferase reporter under the control of the netrin-1 promoter (pGL3-NetP-Luc) or the pGL3 empty vector. All transfections were done in triplicate and the Dual-Luciferase Reporter Assay system (Promega) was performed 48 h after transfection according to the manufacturer's protocol, using the Luminoskan Ascent apparatus. As an internal control of transfection efficiency, the renilla luciferase-encoding plasmid (pRL-CMV; Promega) was cotransfected, and for each sample firefly luciferase activity was normalized to the renilla luciferase activity.

Chicken model for NB progression and dissemination. 10^7 NB cells suspended in 40 µl of complete medium were seeded on 10-d-old chick CAM. 10 µg DCC-5Fbn or the same PBS volume was injected in the tumor on days 11 and 14. For siRNA treatment, 4 µg of scramble or netrin-1 siRNA was injected under the same conditions as for DCC-5Fbn. On day 17, tumors were resected and the area was measured with AxioVision Release 4.6 software (Carl Zeiss, Inc.). To test the effect of DCC-5Fbn on metastasis regression, 3 µg DCC-5Fbn or PBS was injected on days 14 and 15 in a chorioallantoic vessel. To assess metastasis, lungs were harvested from the tumor-bearing embryos and genomic DNA was extracted with a NucleoSpin Tissue kit (Macherey-Nagel). Metastasis was quantified by PCR-based detection of the human Alu sequence using the primers 5′-ACGCCCTGTAATCCCAGCACTT-3′ (sense) and 5′-TCGCCCAGGCTGGAGTGCA-3′ (antisense) with chick GAPDH-specific primers (sense, 5′-GAGGAAAGGTCGCCTGGTGGATCG-3′; antisense, 5′-GGTGAGGACAAGCAGTGAGGAACG-3′) as controls. For both couples of primers, metastasis was assessed by polymerase activation at 95°C for 2 min followed by 30 cycles at 95°C for 30 s, 63°C for 30 s, and 72°C for 30 s. Genomic DNA extracted from lungs of healthy chick embryos was used to determine the threshold between NB cell–invaded and –noninvaded lungs. To monitor apoptosis in primary tumors, primary tumors and surrounding CAM were resected and broken up in lysis buffer and caspase-3 activity was measured using the Caspase 3 CPP32 Fluorimetric Assay kit.

NB metastasis in *nude* mice. 7-wk-old (20–22 g body weight) female athymic nu/nu mice were obtained from Charles River Laboratories. The mice were housed in sterilized filter-topped cages and maintained in a pathogen-free animal facility. IGR-N-91–derived PTX and Myoc cell lines were implanted by i.v. injection of 10^6 cells in 130 µl of PBS into a tail vein (day 0). 20 µg DCC-5Fbn or PBS with equal volume was i.p. injected daily during 22 d. Lungs were harvested on day 23. Lung genomic DNA was extracted with the NucleoSpin Tissue kit, and quantification of human tumor cells in lungs was done by PCR-based detection of the human Alu sequence using the primers 5′-CACCTGTAATCCCAGCACTTT-3′ (sense) and 5′-CCCAGGCTGGAGTGCAGT-3′ (antisense), using 25 ng of genomic DNA as previously described (56). PCR was performed under the following conditions: 95°C for 2 min, 30 cycles at 95°C for 30 s, 65°C for 20 s, and 72°C for 20 s. Quantification of human DNA in mice lungs was based on a standard curve using human genomic DNA isolated from PTX and Myoc cell lines.

Online supplemental material. Fig. S1 associates netrin-1 and DCC expression in NB tumors with their apoptosis and invasion molecular signatures obtained with microarrays. Fig. S2 presents netrin-1 mRNA and protein expression in NB cell lines and shows CLB-VolMo netrin-1–high cell line sensitivity to DCC-5Fbn decoy fragment. In Fig. S3, MYCN and neogenin implication in netrin-1 siRNA-induced cell death is studied, and specificity and efficiency of UNC5H siRNAs are presented at the mRNA, protein, and cellular levels. Online supplemental material is available at http://www.jem.org/cgi/content/full/jem.20082299/DC1.

We thank M.M. Coissieux, C. Guix, M.L. Puiffe, I. Iacono, and S. Bréjon for technical assistance. We thank J. Bouzas, J.G. Delcros, and P. Leissner for excellent support. We thank Dale E. Bredesen for precious advice and text correction.

This work was supported by the Ligue Contre le Cancer (P. Mehlen), the Agence Nationale de la Recherche (P. Mehlen), the Institut National du Cancer (J. Bénard, A. Puisieux, and P. Mehlen), the Société Francaise des Cancers de l'Enfant (J. Bénard), The French Health Minister (J. Bénard and D. Valteau-Couanet), The EU fundings Hermione (P. Mehlen) and APOSYS (P. Mehlen), the Centre National de la Recherche Scientifique, and the Centre Léon Bérard.

The authors have no conflicting financial interests.

Submitted: 14 October 2008
Accepted: 3 March 2009

REFERENCES

1. Mehlen, P., S. Rabizadeh, S.J. Snipas, N. Assa-Munt, G.S. Salvesen, and D.E. Bredesen. 1998. The DCC gene product induces apoptosis by a mechanism requiring receptor proteolysis. *Nature*. 395:801–804.
2. Llambi, F., F. Causeret, E. Bloch-Gallego, and P. Mehlen. 2001. Netrin-1 acts as a survival factor via its receptors UNC5H and DCC. *EMBO J.* 20:2715–2722.
3. Thibert, C., M.A. Teillet, F. Lapointe, L. Mazelin, N.M. Le Douarin, and P. Mehlen. 2003. Inhibition of neuroepithelial patched-induced apoptosis by sonic hedgehog. *Science*. 301:843–846.
4. Stupack, D.G., X.S. Puente, S. Boutsaboualoy, C.M. Storgard, and D.A. Cheresh. 2001. Apoptosis of adherent cells by recruitment of caspase-8 to unligated integrins. *J. Cell Biol.* 155:459–470.
5. Matsunaga, E., S. Tauszig-Delamasure, P.P. Monnier, B.K. Mueller, S.M. Strittmatter, P. Mehlen, and A. Chedotal. 2004. RGM and its receptor neogenin regulate neuronal survival. *Nat. Cell Biol.* 6:749–755.
6. Rabizadeh, S., J. Oh, L.T. Zhong, J. Yang, C.M. Bitler, L.L. Butcher, and D.E. Bredesen. 1993. Induction of apoptosis by the low-affinity NGF receptor. *Science*. 261:345–348.
7. Bordeaux, M.C., C. Forcet, L. Granger, V. Corset, C. Bidaud, M. Billaud, D.E. Bredesen, P. Edery, and P. Mehlen. 2000. The RET

proto-oncogene induces apoptosis: a novel mechanism for Hirschsprung disease. *EMBO J.* 19:4056–4063.

8. Mourali, J., A. Benard, F.C. Lourenco, C. Monnet, C. Greenland, C. Moog-Lutz, C. Racaud-Sultan, D. Gonzalez-Dunia, M. Vigny, P. Mehlen, et al. 2006. Anaplastic lymphoma kinase is a dependence receptor whose proapoptotic functions are activated by caspase cleavage. *Mol. Cell. Biol.* 26:6209–6222.
9. Tauszig-Delamasure, S., L.Y. Yu, J.R. Cabrera, J. Bouzas-Rodriguez, C. Mermet-Bouvier, C. Guix, M.C. Bordeaux, U. Arumae, and P. Mehlen. 2007. The TrkC receptor induces apoptosis when the dependence receptor notion meets the neurotrophin paradigm. *Proc. Natl. Acad. Sci. USA.* 104:13361–13366.
10. Del Rio, G., D.J. Kane, K.D. Ball, and D.E. Bredesen. 2007. A novel motif identified in dependence receptors. *PLoS One.* 2:e463.
11. Mehlen, P., and C. Thibert. 2004. Dependence receptors: between life and death. *Cell. Mol. Life Sci.* 61:1854–1866.
12. Bredesen, D.E., P. Mehlen, and S. Rabizadeh. 2005. Receptors that mediate cellular dependence. *Cell Death Differ.* 12:1031–1043.
13. Serafini, T., S.A. Colamarino, E.D. Leonardo, H. Wang, R. Beddington, W.C. Skarnes, and M. Tessier-Lavigne. 1996. Netrin-1 is required for commissural axon guidance in the developing vertebrate nervous system. *Cell.* 87:1001–1014.
14. Keino-Masu, K., M. Masu, L. Hinck, E.D. Leonardo, S.S. Chan, J.G. Culotti, and M. Tessier-Lavigne. 1996. Deleted in colorectal cancer (DCC) encodes a netrin receptor. *Cell.* 87:175–185.
15. Forcet, C., E. Stein, L. Pays, V. Corset, F. Llambi, M. Tessier-Lavigne, and P. Mehlen. 2002. Netrin-1-mediated axon outgrowth requires deleted in colorectal cancer-dependent MAPK activation. *Nature.* 417:443–447.
16. Ackerman, S.L., L.P. Kozak, S.A. Przyborski, L.A. Rund, B.B. Boyer, and B.B. Knowles. 1997. The mouse rostral cerebellar malformation gene encodes an UNC-5-like protein. *Nature.* 386:838–842.
17. Hong, K., L. Hinck, M. Nishiyama, M.M. Poo, M. Tessier-Lavigne, and E. Stein. 1999. A ligand-gated association between cytoplasmic domains of UNC5 and DCC family receptors converts netrin-induced growth cone attraction to repulsion. *Cell.* 97:927–941.
18. Mehlen, P., and A. Puisieux. 2006. Metastasis: a question of life or death. *Nat. Rev. Cancer.* 6:449–458.
19. Grady, W.M. 2007. Making the case for DCC and UNC5C as tumor-suppressor genes in the colon. *Gastroenterology.* 133:2045–2049.
20. Mazelin, L., A. Bernet, C. Bonod-Bidaud, L. Pays, S. Arnaud, C. Gespach, D.E. Bredesen, J.Y. Scoazec, and P. Mehlen. 2004. Netrin-1 controls colorectal tumorigenesis by regulating apoptosis. *Nature.* 431:80–84.
21. Bernet, A., L. Mazelin, M.M. Coissieux, N. Gadot, S.L. Ackerman, J.Y. Scoazec, and P. Mehlen. 2007. Inactivation of the UNC5C Netrin-1 receptor is associated with tumor progression in colorectal malignancies. *Gastroenterology.* 133:1840–1848.
22. Fearon, E.R., K.R. Cho, J.M. Nigro, S.E. Kern, J.W. Simons, J.M. Ruppert, S.R. Hamilton, A.C. Preisinger, G. Thomas, K.W. Kinzler, et al. 1990. Identification of a chromosome 18q gene that is altered in colorectal cancers. *Science.* 247:49–56.
23. Kinzler, K.W., and B. Vogelstein. 1996. Lessons from hereditary colorectal cancer. *Cell.* 87:159–170.
24. Thiebault, K., L. Mazelin, L. Pays, F. Llambi, M.O. Joly, J.C. Saurin, J.Y. Scoazec, G. Romeo, and P. Mehlen. 2003. The netrin-1 receptors UNC5H are putative tumor suppressors controlling cell death commitment. *Proc. Natl. Acad. Sci. USA.* 100:4173–4178.
25. Shin, S.K., T. Nagasaka, B.H. Jung, N. Matsubara, W.H. Kim, J.M. Carethers, C.R. Boland, and A. Goel. 2007. Epigenetic and genetic alterations in Netrin-1 receptors UNC5C and DCC in human colon cancer. *Gastroenterology.* 133:1849–1857.
26. Evans, A.E., G.J. D'Angio, and J. Randolph. 1971. A proposed staging for children with neuroblastoma. Children's cancer study group A. *Cancer.* 27:374–378.
27. Matthay, K.K., J.G. Villablanca, R.C. Seeger, D.O. Stram, R.E. Harris, N.K. Ramsay, P. Swift, H. Shimada, C.T. Black, G.M. Brodeur, et al. 1999. Treatment of high-risk neuroblastoma with intensive chemotherapy, radiotherapy, autologous bone marrow transplantation, and 13-cis-retinoic acid. Children's Cancer Group. *N. Engl. J. Med.* 341:1165–1173.
28. Valteau-Couanet, D., J. Michon, A. Boneu, C. Rodary, Y. Perel, C. Bergeron, H. Rubie, C. Coze, D. Plantaz, F. Bernard, et al. 2005. Results of induction chemotherapy in children older than 1 year with a stage 4 neuroblastoma treated with the NB 97 French Society of Pediatric Oncology (SFOP) protocol. *J. Clin. Oncol.* 23:532–540.
29. Reale, M.A., M. Reyes-Mugica, W.E. Pierceall, M.C. Rubinstein, L. Hedrick, S.L. Cohn, A. Nakagawara, G.M. Brodeur, and E.R. Fearon. 1996. Loss of DCC expression in neuroblastoma is associated with disease dissemination. *Clin. Cancer Res.* 2:1097–1102.
30. Krause, A., V. Combaret, I. Iacono, B. Lacroix, C. Compagnon, C. Bergeron, S. Valsesia-Wittmann, P. Leissner, B. Mougin, and A. Puisieux. 2005. Genome-wide analysis of gene expression in neuroblastomas detected by mass screening. *Cancer Lett.* 225:111–120.
31. Furne, C., N. Rama, V. Corset, A. Chedotal, and P. Mehlen. 2008. Netrin-1 is a survival factor during commissural neuron navigation. *Proc. Natl. Acad. Sci. USA.* 105:14465–14470.
32. Paradisi, A., C. Maisse, A. Bernet, M. Coissieux, M. Maccarrone, J. Scoazec, and P. Mehlen. 2008. NF-κB regulates netrin-1 expression and affects the conditional tumor suppressive activity of the netrin-1 receptors. *Gastroenterology.* 135:1248–1257.
33. Fitamant, J., C. Guenebeaud, M.M. Coissieux, C. Guix, I. Treilleux, J.Y. Scoazec, T. Bachelot, A. Bernet, and P. Mehlen. 2008. Netrin-1 expression confers a selective advantage for tumor cell survival in metastatic breast cancer. *Proc. Natl. Acad. Sci. USA.* 105:4850–4855.
34. Reale, M.A., G. Hu, A.I. Zafar, R.H. Getzenberg, S.M. Levine, and E.R. Fearon. 1994. Expression and alternative splicing of the deleted in colorectal cancer (DCC) gene in normal and malignant tissues. *Cancer Res.* 54:4493–4501.
35. Meyerhardt, J.A., A.T. Look, S.H. Bigner, and E.R. Fearon. 1997. Identification and characterization of neogenin, a DCC-related gene. *Oncogene.* 14:1129–1136.
36. Cole, S.J., D. Bradford, and H.M. Cooper. 2007. Neogenin: a multifunctional receptor regulating diverse developmental processes. *Int. J. Biochem. Cell Biol.* 39:1569–1575.
37. Rajagopalan, S., L. Deitinghoff, D. Davis, S. Conrad, T. Skutella, A. Chedotal, B.K. Mueller, and S.M. Strittmatter. 2004. Neogenin mediates the action of repulsive guidance molecule. *Nat. Cell Biol.* 6:756–762.
38. Llambi, F., F.C. Lourenco, D. Gozuacik, C. Guix, L. Pays, G. Del Rio, A. Kimchi, and P. Mehlen. 2005. The dependence receptor UNC5H2 mediates apoptosis through DAP-kinase. *EMBO J.* 24:1192–1201.
39. Ferrandis, E., J. Da Silva, G. Riou, and J. Benard. 1994. Coactivation of the MDR1 and MYCN genes in human neuroblastoma cells during the metastatic process in the nude mouse. *Cancer Res.* 54:2256–2261.
40. Link, B.C., U. Reichelt, M. Schreiber, J.T. Kaifi, R. Wachowiak, D. Bogoevski, M. Bubenheim, G. Cataldegirmen, K.A. Gawad, R. Issa, et al. 2007. Prognostic implications of Netrin-1 expression and its receptors in patients with adenocarcinoma of the pancreas. *Ann. Surg. Oncol.* 14:2591–2599.
41. Inbal, B., O. Cohen, S. Polak-Charcon, J. Kopolovic, E. Vadai, L. Eisenbach, and A. Kimchi. 1997. DAP kinase links the control of apoptosis to metastasis. *Nature.* 390:180–184.
42. Stupack, D.G., T. Teitz, M.D. Potter, D. Mikolon, P.J. Houghton, V.J. Kidd, J.M. Lahti, and D.A. Cheresh. 2006. Potentiation of neuroblastoma metastasis by loss of caspase-8. *Nature.* 439:95–99.
43. Yebra, M., A.M. Montgomery, G.R. Diaferia, T. Kaido, S. Silletti, B. Perez, M.L. Just, S. Hildbrand, R. Hurford, F. Florkiewicz, et al. 2003. Recognition of the neural chemoattractant Netrin-1 by integrins alpha6beta4 and alpha3beta1 regulates epithelial cell adhesion and migration. *Dev. Cell.* 5:695–707.
44. Park, K.W., D. Crouse, M. Lee, S.K. Karnik, L.K. Sorensen, K.J. Murphy, C.J. Kuo, and D.Y. Li. 2004. The axonal attractant Netrin-1 is an angiogenic factor. *Proc. Natl. Acad. Sci. USA.* 101:16210–16215.
45. Lu, X., F. Le Noble, L. Yuan, Q. Jiang, B. De Lafarge, D. Sugiyama, C. Breant, F. Claes, F. De Smet, J.L. Thomas, et al. 2004. The netrin receptor UNC5B mediates guidance events controlling morphogenesis of the vascular system. *Nature.* 432:179–186.
46. Nguyen, A., and H. Cai. 2006. Netrin-1 induces angiogenesis via a DCC-dependent ERK1/2-eNOS feed-forward mechanism. *Proc. Natl. Acad. Sci. USA.* 103:6530–6535.

47. Wilson, B.D., M. Ii, K.W. Park, A. Suli, L.K. Sorensen, E. Larrieu-Lahargue, L.D. Urness, W. Suh, J. Asai, G.A. Kock, et al. 2006. Netrins promote developmental and therapeutic angiogenesis. *Science*. 313:640–644.
48. Jiang, Y., L. Min-tsai, and M.D. Gershon. 2003. Netrins and DCC in the guidance of migrating neural Crest-derived cells in the developing bowel and pancreas. *Dev. Biol.* 258:364–384.
49. Roperch, J.P., K. El Ouadrani, A. Hendrix, S. Emami, O. De Wever, G. Melino, and C. Gespach. 2008. Netrin-1 induces apoptosis in human cervical tumor cells via the TAp73alpha tumor suppressor. *Cancer Res.* 68:8231–8239.
50. Bourhis, J., C. Dominici, H. McDowell, G. Raschella, G. Wilson, M.A. Castello, E. Plouvier, J. Lemerle, G. Riou, J. Benard, et al. 1991. N-myc genomic content and DNA ploidy in stage IVS neuroblastoma. *J. Clin. Oncol.* 9:1371–1375.
51. Rubie, H., D. Plantaz, C. Coze, J. Michon, D. Frappaz, M.C. Baranzelli, P. Chastagner, M.C. Peyroulet, and O. Hartmann. 2001. Localised and unresectable neuroblastoma in infants: excellent outcome with primary chemotherapy. Neuroblastoma Study Group, Societe Francaise d'Oncologie Pediatrique. *Med. Pediatr. Oncol.* 36:247–250.
52. Ambros, I.M., J. Benard, M. Boavida, N. Bown, H. Caron, V. Combaret, J. Couturier, C. Darnfors, O. Delattre, J. Freeman-Edward, et al. 2003. Quality assessment of genetic markers used for therapy stratification. *J. Clin. Oncol.* 21:2077–2084.
53. Ghoumari, A.M., R. Wehrle, O. Bernard, C. Sotelo, and I. Dusart. 2000. Implication of Bcl-2 and Caspase-3 in age-related Purkinje cell death in murine organotypic culture: an in vitro model to study apoptosis. *Eur. J. Neurosci.* 12:2935–2949.
54. Vandesompele, J., K. De Preter, F. Pattyn, B. Poppe, N. Van Roy, A. De Paepe, and F. Speleman. 2002. Accurate normalization of real-time quantitative RT-PCR data by geometric averaging of multiple internal control genes. *Genome Biol.* 3:research0034.1–0034.11.
55. Gotoh, T., H. Hosoi, T. Iehara, Y. Kuwahara, S. Osone, K. Tsuchiya, M. Ohira, A. Nakagawara, H. Kuroda, and T. Sugimoto. 2005. Prediction of MYCN amplification in neuroblastoma using serum DNA and real-time quantitative polymerase chain reaction. *J. Clin. Oncol.* 23:5205–5210.
56. Schneider, T., F. Osl, T. Friess, H. Stockinger, and W. Scheuer. 2002. Quantification of human Alu sequences by real-time PCR–an improved method to measure therapeutic efficacy of anti-metastatic drugs in human xenotransplants. *Clin. Exp. Metastasis.* 19:571–582.

Oncogene (2009) 28, 3631–3641

www.nature.com/onc

ORIGINAL ARTICLE

Plk1 regulates liver tumor cell death by phosphorylation of TAp63

S Komatsu[1,2], H Takenobu[1], T Ozaki[1], K Ando[1], N Koida[1], Y Suenaga[1], T Ichikawa[1], T Hishiki[2], T Chiba[3], A Iwama[3], H Yoshida[2], N Ohnuma[2], A Nakagawara[1] and T Kamijo[1]

[1]*Division of Biochemistry, Chiba Cancer Center Research Institute, Chiba, Japan;* [2]*Department of Pediatric Surgery, Graduate School of Medicine, Chiba University, Chiba, Japan and* [3]*Department of Cellular and Molecular Medicine, Graduate School of Medicine, Chiba University, Chiba, Japan*

We previously found that Plk1 inhibited the p53/p73 activity through its direct phosphorylation. In this study, we investigated the functional role of Plk1 in modulating the p53 family member TAp63, resulting in the control of apoptotic cell death in liver tumor cells. Immunoprecipitation and *in vitro* pull-down assay showed that p63 binds to the kinase domain of Plk1 through its DNA-binding region. *in vitro* kinase assay indicated that p63 is phosphorylated by Plk1 at Ser-52 of the transactivating (TA) domain. Plk1 decreased the protein stability of TAp63 by its phosphorylation and suppressed TAp63-induced cell death. Furthermore, Plk1 knockdown in *p53*-mutated liver tumor cells transactivated p53 family downstream effectors, *PUMA*, *p21*$^{Cip1/WAF1}$ and *14-3-3σ*, and induced apoptotic cell death. Double knockdown of Plk1/p63 attenuated Plk1 knockdown-induced apoptotic cell death and transactivation. Intriguingly, both Plk1 and p63 are highly expressed in the side population (SP) fraction of liver tumor cells compared to non-SP fraction cells, suggesting the significance of Plk1/TAp63 in the control of cell death in tumor-initiating SP fraction cells. Thus, Plk1 controls TAp63 by its phosphorylation and regulates apoptotic cell death in liver tumor cells. Plk1/TAp63 may be a suitable candidate as a molecular target of liver tumor treatments.
Oncogene (2009) **28,** 3631–3641; doi:10.1038/onc.2009.216; published online 10 August 2009

Keywords: p63; phosphorylation; Plk1; apoptosis

Introduction

Polo-like kinase 1 (Plk1) is a key regulator of progression through mitosis. Although Plk1 seems to be dispensable for entry into mitosis, its role in spindle formation and exit from mitosis is crucial (Eckerdt and Strebhardt, 2006). Plk1 is overexpressed in human tumors and has prognostic potential in cancer (Strebhardt and Ullrich, 2006). Previously, our laboratory reported that Plk1 is highly expressed in hepatoblastoma samples and patients with a high expression of Plk1 showed significantly poorer prognosis than those with a low expression (Yamada *et al.*, 2004), indicating Plk1's involvement in carcinogenesis and its potential as a therapeutic target in liver cell malignancy. In fact, depletion of Plk1 by small interfering RNA (siRNA) treatment resulted in the arrest of cell-cycle progression at the G2/M phase, such that proliferation was dramatically reduced and apoptosis increased in multiple cancer cell lines (Strebhardt and Ullrich, 2006); however, the downstream effectors and the molecular mechanism of Plk1-depletion-induced apoptosis have not been identified in detail. In the previous paper, we found that Plk1 inhibits the pro-apoptotic function of p53 through physical interaction (Ando *et al.*, 2004) and that Plk1 has the ability to bind to and phosphorylate transactivating (TA)p73 at Thr27, thereby inhibiting its transcriptional as well as pro-apoptotic activity (Koida *et al.*, 2008), suggesting that p53 family molecules have a significant function in Plk1-depletion-induced apoptosis in cancer cells.

The p63 gene has strong homology to the tumor suppressor p53 and the related gene, p73. p63 is actually the oldest evolutionary conserved member of the p53 family phylogenetically (Blandino and Dobbelstein, 2004). It is a tumor suppressor gene and the most frequent site of genetic alterations in human cancers (Vousden and Lu, 2002). p53 protein is a transcription factor that regulates the expression of a wide variety of genes involved in cell-cycle arrest and apoptosis in response to genotoxic or cellular stress (Levine, 1997; Yang *et al.*, 1998). Post-translational modification of p53 families is a key to their regulation. By contrast, reports on p63 phosphorylation are limited and its analysis remains to be confirmed (Westfall *et al.*, 2005; Suh *et al.*, 2006; MacPartlin *et al.*, 2008). In general, many functional parallels are found among p53, TAp73 and TAp63. When ectopically overexpressed in cell culture, TAp63 and TAp73 closely mimic the transcriptional activity and the biological function of p53. In reporter assays, p63/73-responsive promoters include well-known p53 target genes involved in anti-proliferative and pro-apoptotic cellular stress responses such as *p21*$^{Cip1/WAF1}$, *14-3-3σ*, *Bax*, and so on (Candi *et al.*, 2007). Furthermore, both p63 and p73 isoforms contribute to the regulation of cell survival and apoptosis in human

Correspondence: Dr T Kamijo, Division of Biochemistry, Chiba Cancer Center Research Institute, 666-2 Nitona, Chuo-ku, Chiba, Chiba 260-8717, Japan.
E-mail: tkamijo@chiba-cc.jp
Received 27 November 2008; revised 17 June 2009; accepted 23 June 2009; published online 10 August 2009

tumors (Moll and Slade, 2004). Indeed, their ability to regulate apoptosis is clearly a major mechanism by which these genes contribute to human tumorigenesis (Rocco *et al.*, 2006). Initial studies in mice have shown the pro-apoptotic activity of endogenous p63 and p73. Germline deletion of p63 or p73 yielded mouse embryo fibroblasts (MEFs) that were less sensitive to DNA-damage-induced apoptosis than to wild-type cells when transformed by adenoviral E1A protein (Flores *et al.*, 2002). Although the above-mentioned lines of evidence indicate that p63 has an important function in DNA damage, controlling cell-cycle arrest and apoptosis, and in human cancer, its precise role in tumorigenesis remains to be elucidated. For example, unlike p53, p63 is rarely mutated in human cancers (Kato *et al.*, 1999), thus indicating it is not a canonical tumor suppressor. Furthermore, a potential role for p63 in carcinogenesis is supported by the finding of p63 genomic locus amplification and/or overexpression in more than 80% of primary head and neck squamous cell carcinoma as well as in other squamous epithelial cell malignancies (Massion *et al.*, 2003). On the other hand, some tumor types have been reported to lose p63 expression, suggesting the acceleration of tumorigenesis by p63 downregulation (Urist *et al.*, 2002; Koga *et al.*, 2003).

In liver cell malignancy, the precise role of p63 in tumorigenesis and its clinical significance have not been elucidated. Liver cancer ranks fifth in the world among human cancers for incidence and third for mortality (Parkin *et al.*, 2001). Hepatocellular carcinoma (HCC), the most common malignant tumor of the liver, has an extremely unfavorable prognosis (over 95% mortality after 5 years), because of, in particular, the resistance of HCC cells to chemotherapy or radiotherapy (Bruix and Llovet, 2002). A high incidence of p53 mutation is observed in developing countries (53%; Shen and Ong, 2004), although p53 missense mutations are observed in ~25% of HCC samples from industrialized countries, where the tumor essentially develops from alcohol-generated cirrhosis (Montesano *et al.*, 1997). Previous reports indicated that the expression of TAp63 and deltaNp63 in HCC cell lines and the upregulation of TAp63 in response to certain forms of DNA damage accompanied with the increase in p53 target gene transcription (Petitjean *et al.*, 2005) and treatment of HCC with chemotherapeutic drugs resulted in a dramatic increase in TAp63alpha levels (Gressner *et al.*, 2005).

In this study, we have found that Plk1 directly binds to TAp63alpha and phosphorylates TAp63 at the Ser-52, resulting in inhibition of its transcriptional activities caused by acceleration of protein degradation. To the best of our knowledge, this is the first report to determine the phosphorylated serine residue in the TA domain of p63. Plk1-depletion-induced apoptosis and activated p53 pathway downstream effectors are partially cancelled by p63 depletion in HCC cells. Furthermore, our finding suggests the possibility that Plk1/p63 appears to be an important candidate for cancer stem-cell-targeted therapy in liver cell malignancy.

Results

Physical and functional interaction between Plk1 and p63

First, we examined whether Plk1 interacts with TAp63. COS-7 cells were transiently transfected with the expression plasmid for FLAG-tagged Plk1 and/or HA-tagged TAp63alpha. Whole-cell lysates prepared from transfected cells were immunoprecipitated with a monoclonal anti-HA antibody, and the immunoprecipitates were analysed by immunoblotting with a monoclonal anti-FLAG antibody. As shown in Figure 1a, FLAG-Plk1 was co-immunoprecipitated with HA-TAp63, and the analysis of the anti-FLAG immunoprecipitates also showed that HA-TAp63 is co-immunoprecipitated with FLAG-Plk1.

Furthermore, endogenous interaction between Plk1 and p63 was also detected using HaCaT cells (Figure 1b). These results indicate that Plk1 interacts with p63 in mammalian cultured cells. As HaCaT cells show a high expression level of deltaNp63, this

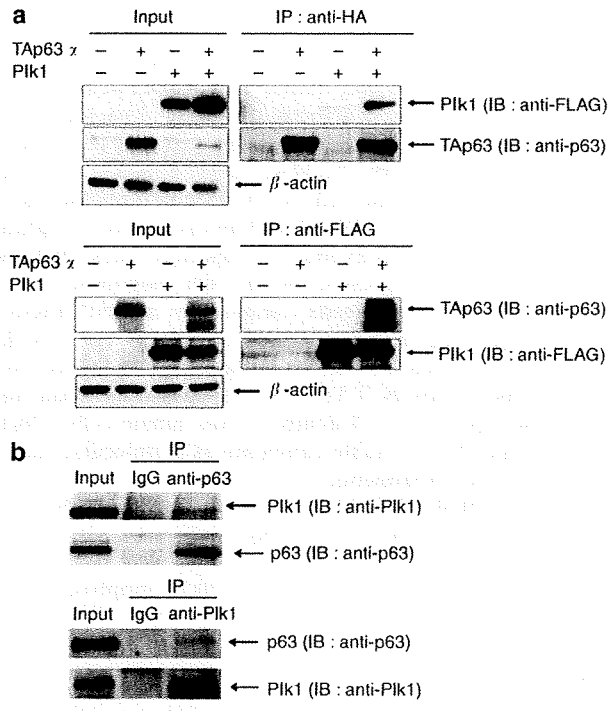

Figure 1 Interaction between Plk1 and p63 in cells. (**a**) Interaction between exogenously expressed Plk1 and TAp63. Whole-cell lysates from COS-7 cells transfected with FLAG-Plk1 and/or HA-TAp63 expression plasmids were immunoprecipitated with monoclonal anti-HA antibody (clone 3F10, Roche) and monoclonal anti-FLAG antibody (clone M2, Sigma), and immunoblotted with monoclonal anti-FLAG antibody and monoclonal anti-p63 antibody (clone 4a4) as indicated, to observe the interaction. Control immunoprecipitation experiments and loading control β-actin signals were also indicated. (**b**) Interaction between endogenous Plk1 and p63. A total of 500 μg of nuclear extract from HaCaT cells were immunoprecipitated with IgG, monoclonal anti-63 antibody (clone 4A4) or monoclonal anti-Plk1 antibody and subjected to SDS–PAGE (polyacrylamide gel electrophoresis) and protein transfer. The transferred membranes were immunoblotted with monoclonal anti-Plk1 antibody or monoclonal anti-p63 (clone 4a4) antibody to observe the interaction. *IgG*, mouse IgG.

interaction was supposed to be between Plk1 and deltaNp63.

TAp63 binds to the kinase domain of Plk1 through its DNA-binding region

Next, to map the p63-interacting domain on Plk1, we constructed FLAG-tagged Plk1 deletion mutants, including Plk1-(1–401), Plk1-(1–329) and Plk1-(1–98) (Figure 2a). We then tested the interaction between TAp63alpha and each of these Plk1 deletion mutants. COS-7 cells were transfected with the expression plasmid encoding TAp63alpha and each Plk1 deletion mutant, and co-immunoprecipitation experiments were carried out to determine the interaction.

We found that Plk1-(1–401) and Plk1-(1–329) retained the ability to bind to TAp63alpha, whereas Plk1-(1–98) did not (Figure 2b). These results indicate that Plk1 physically interacts with TAp63alpha through its 99–329 amino acid residues. To identify the essential region of TAp63alpha required for the interaction with Plk1, we carried out *in vitro* pull-down assays. The indicated glutathione-*S*-transferase (GST)–TAp63alpha deletion mutants (Figure 2c) were purified with glutathione-sepharose beads. Each of these GST fusion proteins was incubated with radiolabeled FLAG-Plk1, which was generated by the *in vitro* transcription/translation system in the presence of [^{35}S]methionine. As clearly shown in Figure 2d, radiolabeled FLAG-Plk1 was efficiently pulled down by GST–TAp63alpha-(282–357), implying that the region between amino acid residues 282 and 353 of TAp63alpha is important for the interaction with Plk1. As this binding site is common between TAp63 and deltaNp63, in Figure 1b, it is believed that Plk1 binds to TAp63 as well as to deltaNp63.

Plk1 directly phosphorylates Ser-52 of TAp63

Furthermore, to address whether Plk1 could phosphorylate TAp63, we carried out an *in vitro* kinase reaction. GST and GST–TAp63alpha fusion proteins were incubated with the active form of Plk1 in the presence of [γ^{32}P]ATP. The reaction mixtures were separated by SDS–polyacrylamide gel electrophoresis (PAGE) and subjected to autoradiography (Figure 3a). The results suggested that Plk1 phosphorylates the region between amino acid residues 20 and 96 of TAp63.

As described earlier (Nakajima *et al*., 2003), a sequence (D/E)*X*(S/T)ΦD/E) (where *X* is any amino acid and Φ a hydrophobic amino acid) was identified as a consensus motif for Plk1-dependent phosphorylation. According to the search for a putative phosphorylation site targeted by Plk1 within the amino acid sequence of TAp63 (residues 20–96), we identified related motifs, (39EPSEDG44 and 50EISMDC55), in the NH2-terminal portion of TAp63alpha (Figure 3b).

To further confirm whether Ser-41 or Ser-52 of TAp63 could be phosphorylated by Plk1, we generated a mutant form of GST-p63-(1–102), termed as 'S41A' and 'S52A,' where Ser-41 or Ser-52 was substituted to Ala. Purified GST fusion proteins were subjected to the *in vitro* kinase reaction. As shown in Figure 3c, GST–TAp63-(1–102) and S41A mutant were strongly radiolabeled in the presence of Plk1, whereas S52A mutant was not labeled, indicating that Ser-52 of TAp63 is at least one of the phosphorylation sites targeted by Plk1, and is located in the transcriptional domain of TAp63. In addition, it seemed to be interesting that the molecular size of the mutant p63(1–102)S52A was smaller than that of p63 (1–102)S41A and p63(1–102), suggesting the effect of phosphorylation of S52 of TAp63 on the molecular weight of the 1–102 peptide.

Plk1 represses TAp63-mediated transcriptional activation

To address the effect of Plk1 on the transcriptional activity of TAp63, we carried out luciferase reporter assays. H1299 cells were co-transfected with a constant amount of the expression plasmid for TAp63alpha, the luciferase reporter construct carrying p53/p63-responsive *p21$^{Cip1/WAF1}$*, *BAX* or *MDM2* promoter and *Renilla* luciferase cDNA (pRL-TK) together with or without increasing amounts of FLAG-Plk1 expression plasmid. Enforced expression of FLAG-Plk1 significantly reduced luciferase activities driven by the indicated promoters in a dose-dependent manner (Figure 4a). These results suggest that Plk1 has the ability to repress the transcriptional activity of TAp63. Furthermore, to examine whether the kinase activity of Plk1 could be necessary for the inhibition of TAp63 function, we tested the possible effect of the kinase-deficient mutant form of Plk1, Plk1(K82M) (Supplementary data) on TAp63. For this purpose, we first examined whether Plk1(K82M) could interact with TAp63 in cells. The interaction between TAp63alpha and Plk1(K82M) was confirmed bi-directionally (Figure 4b). These results suggest that the kinase-deficient mutant form of Plk1 retains the ability to interact with TAp63 in cells. To further examine the effect of the kinase activity of Plk1 on TAp63 function, we carried out luciferase reporter assays. H1299 cells were co-transfected with a constant amount of the expression plasmid for TAp63alpha, a luciferase reporter construct bearing p53/p63-responsive *p21$^{Cip1/WAF1}$*, *BAX* or *MDM2* promoter and *Renilla* luciferase cDNA together with or without increasing amounts of FLAG-Plk1(K82M). As shown in Figure 4c, FLAG-Plk1(K82M) had a negligible effect on the transcriptional activity of TAp63. Collectively, these results indicate that kinase activity of Plk1 is required for the inhibition of TAp63 function.

Plk1 reduces the protein stability of TAp63 by its phosphorylation and suppresses TAp63-induced cell death

Next, we checked the effect of Plk1 on TAp63-induced cell death. H1299 cells were transfected with mock, TAp63alpha, TAp63alpha/Plk1 or TAp63alpha/KD Plk1, and at 24 h after transfection, the cells were observed. TAp63alpha-transfected cells showed the inhibition of cell growth and increase in shrunken and floating cells compared with mock transfection;

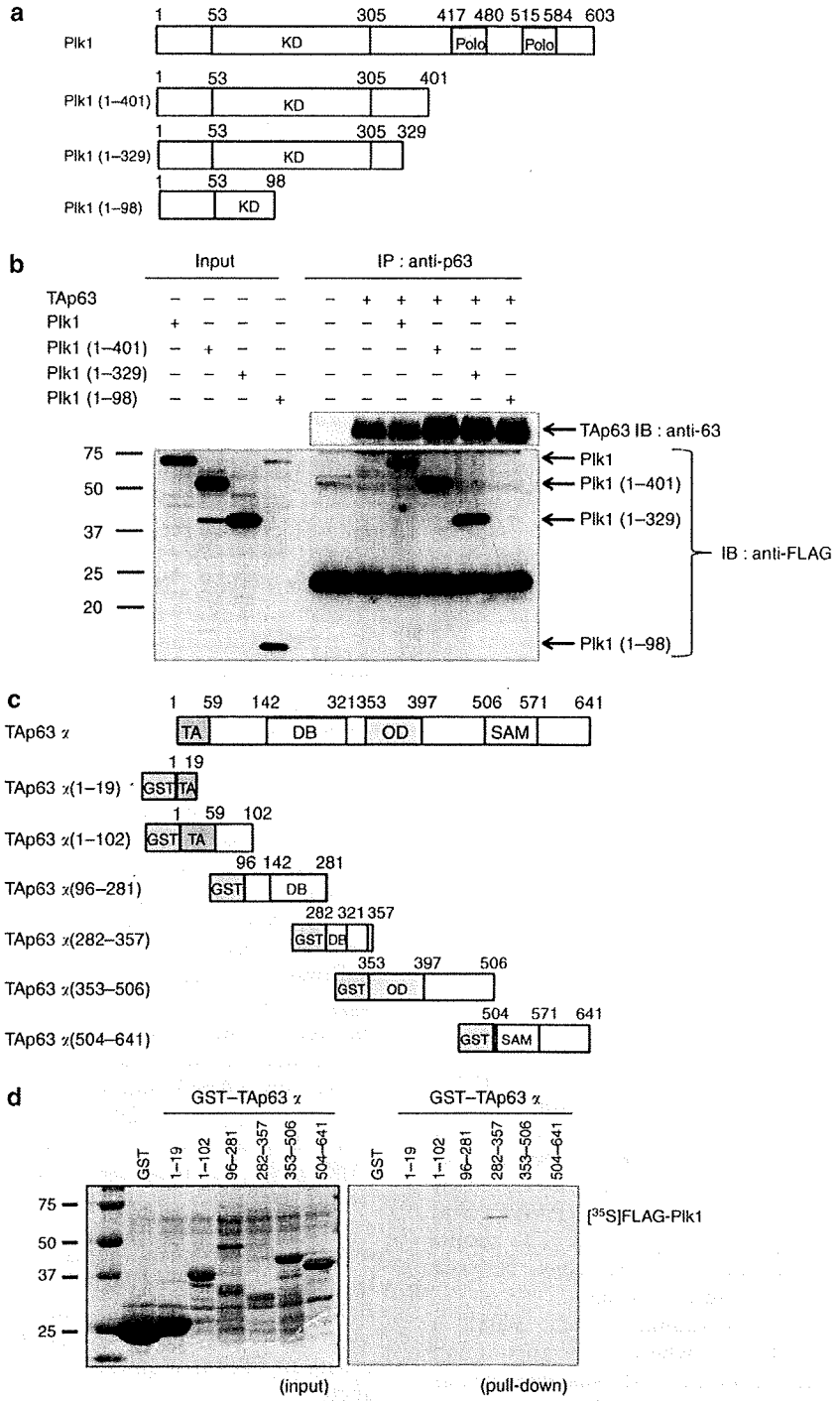

Figure 2 TAp63 binds to the kinase domain of Plk1 through its DNA-binding region. **(a)** Schematic representation of Plk1 deletion mutants. *KD*, kinase domain; *Polo*, polo-box; numbers indicate amino acid position. **(b)** Interaction between Plk1 deletion mutants and TAp63. Whole-cell lysates from COS-7 cells transfected with the indicated expression plasmids were immunoprecipitated with monoclonal anti-p63 antibody and immunoblotted with monoclonal anti-FLAG antibody to observe the interaction between Plk1 deletion mutants and TAp63. Immunoprecipitation with mouse IgG was used as a negative control. Equal amounts of protein derived from cell lysates were immunoblotted with monoclonal anti-FLAG antibody. Control immunoprecipitation–immunoblotting experiments of TAp63 were also indicated. **(c)** Domain structure of wild-type TAp63alpha and a schematic representation of GST-tagged TAp63alpha deletion mutants. *TA*, transactivation domain; *DB*, DNA-binding domain; *OD*, oligomerization domain; *SAM*, sterileá-motif domain. Numbers indicate amino acid positions. **(d)** *In vitro* pull-down assay. An equal amount of radiolabeled FLAG-Plk1 was incubated with GST or GST–TAp63alpha fusion proteins. After incubation, GST or GST–TAp63alpha fusion proteins was recovered by glutathione-Sepharose beads, and bound materials were resolved by 10% SDS–PAGE (polyacrylamide gel electrophoresis) followed by autoradiography.